(RISM), an integral equation approach originally introduced by Chandler and Andersen (Chandler, 1982).

9.2 Elements of Integral Equation Theory for Simple Fluids

The Ornstein-Zernike equation, Eq. (9.46), is an integral equation in two unknown functions, $h(r)$ and $c(r)$. If one introduces a judicious approximation relating $h(r)$ and $c(r)$, one can convert the Ornstein- Zernike into an integral equation in one unknown function. By solving this integral equation, one can obtain the structure of the fluid ($h(r)$, therefore $g(r)$) at given density ρ and temperature T, hence the fluid's thermodynamic properties.

Such an additional equation connecting $h(r)$ and $c(r)$ is said to provide *closure* to the Ornstein-Zernike equation. The system of the Ornstein- Zernike and the closure equation constitutes an *integral equation theory* for the fluid structure.

Closure equations can be arrived at by detailed analysis of the graphical expansions of $g(r)$ and $h(r)$, or through formulations that employ the theory of functionals. Here we will only present a heuristic justification of the *Percus-Yevick* closure, originally derived through a very different argument [Percus and Yevick (1958)]. Our brief discussion follows mainly McQuarrie [McQuarrie (1979), Chapter 13].

9.2.1 The Percus-Yevick Approximation

To justify the Percus-Yevick closure, it is useful to think of the direct correlation function as a difference:

$$c(r) \simeq g_{total}(r) - g_{indirect}(r)$$

By Eq. (9.37), we can express $g_{total}(r)$ in terms of the potential of mean force $w(r)$ as

$$g_{total}(r) \equiv g(r) = \exp\left[-\beta\, w(r)\right]$$

Furthermore, it would make sense to associate the indirect part of the pair distribution function with a potential $w(r) - \mathcal{V}_{pair}(r)$, as $w(r)$ is the potential of mean force governing total correlations and $\mathcal{V}_{pair}(r)$ is the pair potential governing direct correlations in the fluid:

$$g_{indirect}(r) = \exp\left[-\beta\{w(r) - \mathcal{V}_{pair}(r)\}\right]$$

Combining the above three relations,

$$c(r) \simeq g(r) - g(r)\, \exp\left[\beta\, \mathcal{V}_{pair}(r)\right]$$

This connection between $c(r)$ and $g(r)$ is the Percus-Yevick (PY) approximation. It is convenient to introduce the function

$$y(r) = \exp\left[\beta \mathcal{V}_{pair}(r)\right]\, g(r) \tag{9.50}$$

The PY approximation can be written in the following alternative forms:

$$c(r) = \left[1 - \exp\{\beta \mathcal{V}_{pair}(r)\}\right]\, g(r) =$$

$$[1 - \exp\{\beta \mathcal{V}_{pair}(r)\}]\ [h(r) + 1] =$$

$$[\exp\{-\beta \mathcal{V}_{pair}(r)\} - 1]\ y(r) \tag{9.51}$$

9.2.2 Some properties of $y(r) = \exp[\beta \mathcal{V}_{pair}(r)]\ g(r)$. Relation between pressure and contact pair distribution function in a hard sphere fluid

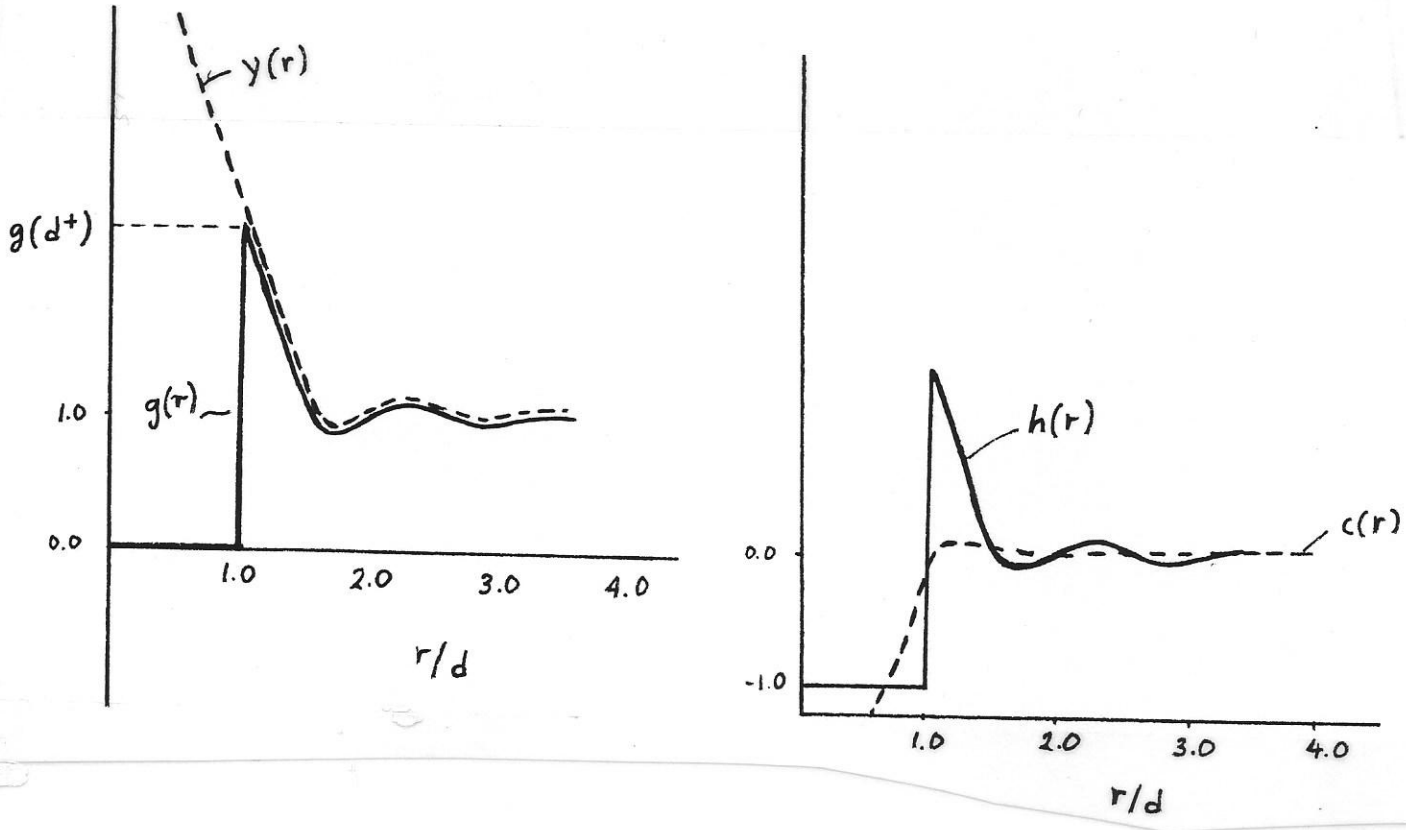

Figure 9.10 The functions $g(r)$, $y(r)$, $h(r)$, and $c(r)$ in a hard sphere system at a typical liquid density. The function $y(r)$ is continuous at $r = d$, the hard-sphere diameter. The contact value of the pair distribution function, $g(d^+)$, is shown.

There are two incentives for introducing the distribution function $y(r)$, defined through Eq. (9.50). First, $y(r)$ is not very sensitive to the exact form of the pair potential $\mathcal{V}_{pair}(r)$; thus, using an approximate expression for $y(r)$ within an integral equation

or perturbation theory is not likely to degrade the quality of the results. Second, unlike the functions $g(r)$ and $h(r)$, which are discontinuous for hard sphere systems at a value of r equal to the hard sphere diameter d, the function $y(r)$ is smooth even when the potential is discontinuous. Multiplication by the Boltzmann factor of the discontinuous pair potential in Eq. (9.50) removes, in a sense, the discontinuity in $g(r)$ caused by that potential. This is seen characteristically in Figure 9.10, which displays the distance dependence of the functions $g(r), h(r), c(r)$, and $y(r)$ in a hard-sphere system.

As an application of the continuity of $y(r)$ we consider the calculation of pressure in a hard-sphere fluid. The applicability of the pressure equation, Eq. (9.34), is limited by the discontinuous nature of the pair potential. Substituting $g(r)$ in terms of $y(r)$, we obtain

$$\frac{\beta P}{\rho} = 1 - \frac{2\pi}{3}\beta\rho \int_0^\infty \frac{\partial \mathcal{V}_{pair}}{\partial r}\, g(r)\, r^3\, dr =$$

$$= 1 - \frac{2\pi}{3}\beta\rho \int_0^\infty \frac{\partial \mathcal{V}_{pair}}{\partial r}\, y(r)\, \exp\left[-\beta \mathcal{V}_{pair}\right]\, r^3\, dr =$$

$$= 1 + \frac{2\pi}{3}\rho \int_0^\infty r^3\, y(r)\, \frac{\partial}{\partial r}\left\{\exp\left[-\beta \mathcal{V}_{pair}\right]\right\}\, dr$$

For the hard sphere fluid, $\exp\left[-\beta \mathcal{V}_{pair}\right]$ is a Heaviside step function at $r = d$. Its derivative will be a Dirac delta function at $r = d$. Then,

$$\frac{\beta P}{\rho} = 1 + \frac{2\pi}{3}\rho \int_0^\infty r^3\, y(r)\, \delta(r - d)\, dr =$$

$$1 + \frac{2\pi}{3}\rho \lim_{r \to d} \left[r^3\, y(r)\right] + 1 + \frac{2\pi}{3}\rho \lim_{r \to d+} \left[d^3\, g(r)\right]$$

where the notation $\lim_{r \to d+}$ signifies that d is approached from larger r values.

$$\frac{\beta P^{HS}}{\rho} = 1 + \frac{2}{3}\pi \rho d^3 \lim_{r \to d+} g_{HS}(r) \equiv 1 + \frac{2}{3}\pi \rho d^3 g_{HS}(d^+) \tag{9.52}$$

Eq. (9.52) is an important relation connecting the pressure of a hard-sphere system to the value of the pair distribution function at contact.

9.2.3 The Percus-Yevick Solution for Hard Spheres. Carnahan- Starling Equation of State

In this section we briefly examine the application of the PY integral equation theory to the hard-sphere fluid. The hard-sphere diameter d is the only potential parameter governing interactions in this fluid. A schematic representation of the pair potential is given in Figure 9.7, with $\sigma \equiv d$. The structure of the hard-sphere system is dictated entirely by its density ρ, or, equivalently, by the *packing fraction*

$$\eta = \rho \frac{\pi}{6} d^3 = \frac{\text{Volume of molecules}}{\text{volume of system}} \tag{9.53}$$

There is an upper limit to the packing fraction, which corresponds to a face centered cubic (fcc) crystal with all molecules in contact:

$$\eta_{max} = \frac{\pi}{3(2^{1/2})} = 0.74 \quad (\text{or } \rho d^3 = 2^{1/2})$$

The hard-sphere system exhibits a fluid-solid phase transition (crystallization). The packing fractions of the two phases coexisting at equilibrium at this first order phase transition are

$$\eta_{fluid} = 0.49 \quad (\rho d^3 = 0.94)$$

$$\eta_{solid} = 0.55 \quad (\rho\, d^3 = 1.05)$$

There is no gas-liquid phase transition in this system, as attractive forces are absent.

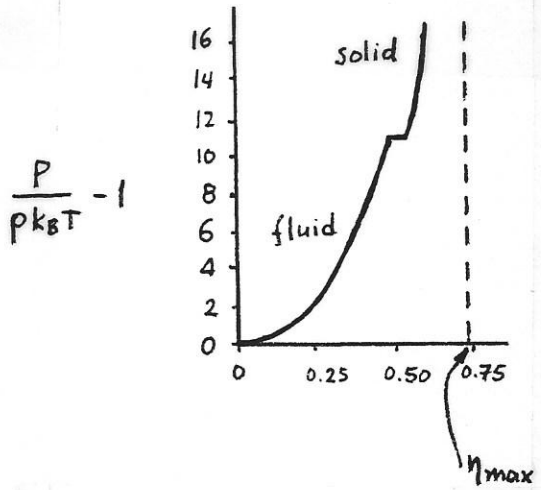

Figure 9.11 Phase diagram for the hard-sphere substance

Figure 9.11 shows the phase diagram of the hard sphere system. It is remarkable that this diagram can be displayed completely on a two-dimensional graph of $\frac{P}{\rho\, k_B\, T}$ *vs.* η, rather than the usual three-dimensional (P, ρ, T) representation. Pressure and temperature effects can be collapsed on a single axis, and this stems from the absence of a characteristic interaction energy scale in this system. That a scaling of the type $\frac{P}{\rho\, k_B\, T} = f(\eta)$ is followed can be readily deduced by dimensional analysis of the canonical partition function of the hard-sphere system.

The following analysis aims at calculating the structure (*i.e.*, the functions $c(r)$, $h(r)$, $g(r)$) for the hard - sphere system in the *fluid* region by invoking the PY approximation. The thermodynamic properties of the fluid will then be obtained through their relationship to $g(r)$ (see sections 9.1.5 and 9.2.1).

For hard spheres, the PY approximation becomes

$$c(r) = [\exp\{-\beta \mathcal{V}_{pair}(r)\} - 1]\, y(r) = \begin{cases} -y(r), & \text{if } r < d \\ 0, & \text{if } r \geq d \end{cases} \tag{9.54}$$

From the relationship between $y(r)$ and $g(r)$, Eq. (9.50), one obtains

$$g(r) = \begin{cases} 0, & \text{if } r < d \\ y(r), & \text{if } r \geq d \end{cases} \tag{9.55}$$

Note that Eqs. (9.55) are exact, stemming from the definition of $y(r)$, while Eqs. (9.54) are approximate, resulting from the PY closure. As a consequence of Eq. (9.55), one has the exact relationship

$$h(r) = \begin{cases} -1, & \text{if } r < d \\ y(r) - 1, & \text{if } r \geq d \end{cases} \tag{9.56}$$

Thus, all three functions $c(r), g(r), h(r)$ that we introduced for the description of structure in a fluid have been expressed in terms of $y(r)$. The Ornstein-Zernike equation, Eq. (9.46), applied for distances $r_{12} > d$, after substitution of c and h in terms of y via Eqs. (9.54) and (9.56), gives

$$y(r_{12}) - 1 = 0 + \rho \int\limits_{\substack{r_{13}<d \\ r_{32}\leq d}} [-y(r_{13})]\,[-1]\, d^3 r_3 + \rho \int\limits_{\substack{r_{13}<d \\ r_{32}>d}} [-y(r_{13})]\,[y(r_{32}) - 1]\, d^3 r_3 + 0 =$$

$$\rho \int\limits_{\substack{r_{13}<d \\ r_{32}\leq d}} y(r_{13})\, d^3 r_3 + \rho \int\limits_{\substack{r_{13}<d \\ r_{32}>d}} y(r_{13})\, d^3 r_3 - \rho \int\limits_{\substack{r_{13}<d \\ r_{32}>d}} y(r_{13})\, y(r_{32})\, d^3 r_3 =$$

$$\rho \int\limits_{r_{13}<d} y(r_{13})\, d^3 r_3 - \rho \int\limits_{\substack{r_{13}<d \\ r_{32}>d}} y(r_{13})\, y(r_{32})\, d^3 r_3 \tag{9.57}$$

Setting $\mathbf{r}_{12} = \mathbf{r}$, $\mathbf{r}_{13} = \mathbf{r}'$, and therefore $\mathbf{r}_{32} = \mathbf{r} - \mathbf{r}'$, Eq. (9.57) can also be written

$$y(r) = 1 + \rho \int\limits_{r'<d} y(r')\, d^3 r' - \rho \int\limits_{\substack{r'<d \\ |\mathbf{r}-\mathbf{r}'|>d}} y(r')\, y(|\mathbf{r} - \mathbf{r}'|)\, d^3 r' \tag{9.58}$$

Eq. (9.58) is an integral equation in the function $y(r)$. Its analytical solution is possible through Laplace transform methods. A relatively straightforward solution procedure, relying on Wiener-Hopf factorization, is given in Hansen and McDonald (1986), Appendix B. Here we will only present the result. The direct correlation function $c(r)$ is

$$c(r) = \begin{cases} -\lambda_1 - 6\,\eta\,\lambda_2 \left(\frac{r}{d}\right) - \frac{1}{2}\,\eta\,\lambda_1 \left(\frac{r}{d}\right)^3 \equiv -y(r) & \text{if } r < d \\ 0 & \text{if } r \geq d \end{cases}$$

where

$$\lambda_1 = \frac{(1+2\eta)^2}{(1-\eta)^4}, \quad \lambda_2 = -\frac{\left(1+\frac{1}{2}\eta\right)^2}{(1-\eta)^4} \tag{9.59}$$

and $\eta = \rho\frac{\pi}{6}\,d^3$ is the packing fraction. Note that the structure of the fluid depends on density, but not on temperature.

There are two pathways for obtaining the equation of state of the hard sphere fluid from the structural result of the Percus-Yevick analysis, Eq. (9.59). The first is to use the hard-sphere pressure equation, Eq. (9.52). From the PY solution,

$$g(d^+) = y(d) = \lambda_1 + 6\,\eta\,\lambda_2 + \frac{1}{2}\,\eta\,\lambda_1 = \frac{1+\frac{1}{2}\eta}{(1-\eta)^2}$$

hence

$$\frac{\beta\,P^v}{\rho} = 1 + 4\,\eta\,g(d^+) = 1 + 4\,\eta\,\frac{1+\frac{1}{2}\eta}{(1-\eta)^2}\ , \quad \text{or}$$

$$\frac{\beta\,P^v}{\rho} = \frac{1+2\,\eta+3\,\eta^2}{(1-\eta)^2} \tag{9.60}$$

where the superscript v denotes that P has been obtained via the virial, or pressure equation.

The second pathway to the equation of state is to use the compressibility equation, Eq. (9.49), in order to obtain κ_T, and then integrate κ_T from zero density (ideal gas state) to the density of interest, to obtain pressure. Using Eq. (9.59) in Eq. (9.49), we obtain

$$1 - \frac{1}{\rho\, k_B T\, \kappa_T} = -\rho\, d^3 \int_0^1 4\pi\, x^2\, dx \left[\lambda_1 + 6\,\eta\,\lambda_2\, x + \frac{1}{2}\,\eta\,\lambda_1\, x^3\right] =$$

$$-\rho\, d^3\, 4\pi \left[\frac{\lambda_1}{3} + 6\,\lambda_2\,\eta\,\frac{1}{4} + \frac{1}{2}\,\eta\,\lambda_1\,\frac{1}{6}\right] = -4\pi\, d^3\,\rho \left[\frac{\lambda_1}{3}\left(1 + \frac{\eta}{4}\right) + \frac{3}{2}\,\eta\,\lambda_2\right] =$$

$$-24\,\eta \left[-\frac{\eta^3 - 4\,\eta^2 + 2\,\eta - 8}{24\,(1-\eta)^4}\right] = \frac{\eta^4 - 4\,\eta^3 + 2\,\eta^2 - 8\,\eta}{(1-\eta)^4} \quad , \quad \text{or}$$

$$\frac{1}{\rho\, k_B T\, \kappa_T} = 1 - \frac{\eta^4 - 4\,\eta^3 + 2\,\eta^2 - 8\,\eta}{(1-\eta)^4} = \frac{1 + 4\,\eta + 4\,\eta^2}{(1-\eta)^4} \quad , \quad \text{or, since} \quad \frac{1}{\kappa_T} = \rho\left(\frac{\partial P}{\partial \rho}\right)_T \quad ,$$

$$\beta\left(\frac{\partial P}{\partial \rho}\right)_T = \frac{1 + 4\,\eta + 4\,\eta^2}{(1-\eta)^4} \quad , \quad \text{or} \quad \beta\left(\frac{\pi}{6}\, d^3\right)\left(\frac{\partial P}{\partial \eta}\right)_T = \frac{1 + 4\,\eta + 4\,\eta^2}{(1-\eta)^4} \quad , \quad \textit{or}$$

$$\beta\left(\frac{\pi}{6}\, d^3\right)\left(\frac{\partial P}{\partial \eta}\right)_T = \frac{1 + 4\,\eta + 4\,\eta^2}{(1-\eta)^4} = \frac{4}{(1-\eta)^2} - \frac{12}{(1-\eta)^3} + \frac{9}{(1-\eta)^4} \quad , \quad \text{or}$$

$$\int_0^\eta \beta\left(\frac{\pi}{6}\, d^3\right)\left(\frac{\partial P}{\partial \eta}\right)_T d\eta = \int_0^\eta \frac{4}{(1-\eta)^2} d\eta - 12 \int_0^\eta \frac{1}{(1-\eta)^3} d\eta + 9 \int_0^\eta \frac{1}{(1-\eta)^4} d\eta =$$

$$\left[-\frac{4}{1-\eta} + 4 + \frac{12}{2\,(1-\eta)^2} - \frac{12}{2} - \frac{9}{3\,(1-\eta)^3} + \frac{9}{3}\right] = \frac{\eta^3 + \eta^2 + \eta}{(1-\eta)^3} \quad , \quad \text{or}$$

$$\beta\left(\frac{\pi}{6}\, d^3\right) P = \eta \frac{1 + \eta + \eta^2}{(1-\eta)^3} = \rho\left(\frac{\pi}{6} d^3\right) \frac{1 + \eta + \eta^2}{(1-\eta)^3} \quad , \quad \text{or}$$

$$\frac{\beta\, P^c}{\rho} = \frac{1 + \eta + \eta^2}{(1-\eta)^3} \tag{9.61}$$

where the superscript c signifies that P has been obtained on the basis of the compressibility equation.

It is remarkable that the two equations of state, obtained via the pressure equation [Eq. (9.60)] and via the compressibility equation [Eq. (9.61)], are *not equivalent* (see

also the graphical representations of these equations in Figure 9.12). This is because the Percus-Yevick closure, which is the only approximation invoked, has introduced some thermodynamic inconsistency into the problem of calculating the properties of the hard sphere fluid.

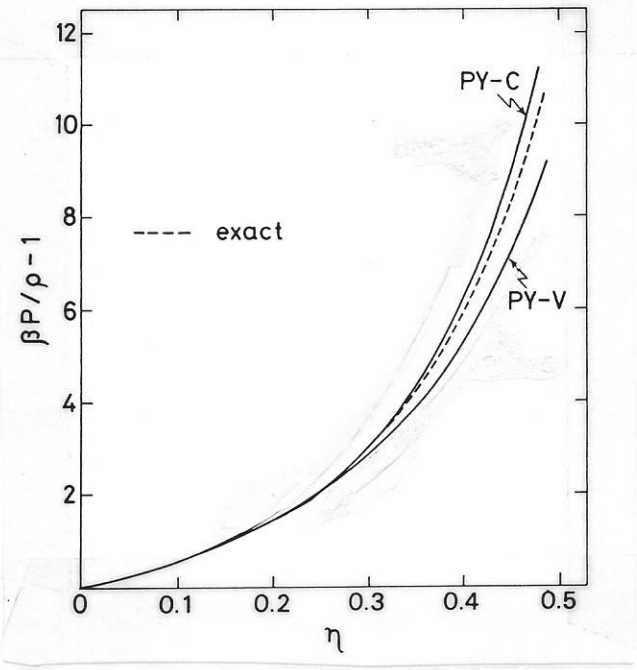

Figure 9.12 Graphical representation of the equations of state obtained from the Percus-Yevick integral equation theory for hard spheres. $PY - v$: P^v from the pressure equation, Eq. (9.60). $PY - c$: P^c from the compressibility equation, Eq. (9.61). The predictions of the Carnahan- Starling equation, Eq. (9.62), practically coincide with the exact results from computer simulation.

Exact results for the equation of state of the hard sphere fluid have been obtained through simulations. The compressibility equation, Eq. (9.61), overestimates P, whereas the pressure equation, Eq. (9.60), underestimates it. Through a clever observation of the virial expansion for hard spheres, Carnahan and Starling were able to devise a simple and accurate equation of state that is in excellent agreement with simulation results

[carnahan and Starling (1969)]. The *Carnahan-Starling* equation of state is

$$\frac{\beta P}{\rho} = \frac{1 + \eta + \eta^2 - \eta^3}{(1-\eta)^3} \tag{9.62}$$

The Carnahan-Starling equation can be thought of as arising through an averaging of the compressibility and virial expressions of the Percus-Yevick treatment with relative weights of 2/3 and 1/3, respectively:

$$\frac{\beta P}{\rho} = \frac{\beta}{\rho}\left(\frac{2}{3}P^c + \frac{1}{3}P^v\right) \tag{9.63}$$

The Carnahan-Starling equation essentially solves the problem of expressing the equation of state of the hard-sphere fluid analytically.

9.2.4 A note on the numerical solution of integral equation theories

It is the exception, rather than the rule, that an analytic solution to an integral equation theory can be found. Iterative schemes for the numerical determination of the solution to an integral equation theory are thus necessary.

As we have seen in the Percus-Yevick example, the system formed by the Ornstein-Zernike equation and the closure relation can be cast as an integral equation in one unknown correlation function, such as $c(r)$ or $h(r)$. For the numerical solution of this integral equation, the r-domain of interest ($0 \leq r \leq r_{max}$, where r_{max} is sufficiently large for correlation functions to have decayed to 0) is subdivided into N equal intervals by defining N points $\{r_i\}$, $r_i = i\,\delta r$, $i = 1(1)N$, $r_N = r_{max}$ (see Fig. 9.13(a)). N is typically chosen to be a power of 2 (*e.g.*, $N = 1024$) to facilitate Fast Fourier Transform

(FFT) computations. With this discretization, the unknown functions $h(r)$ and $c(r)$ can be regarded as vectors, whose determination is the objective of the integral equation:

$$\mathbf{h} \equiv [h(r_1), \ldots, h(r_i), \ldots, h(r_N)]$$

$$\mathbf{c} \equiv [c(r_1), \ldots, c(r_i), \ldots, c(r_N)]$$

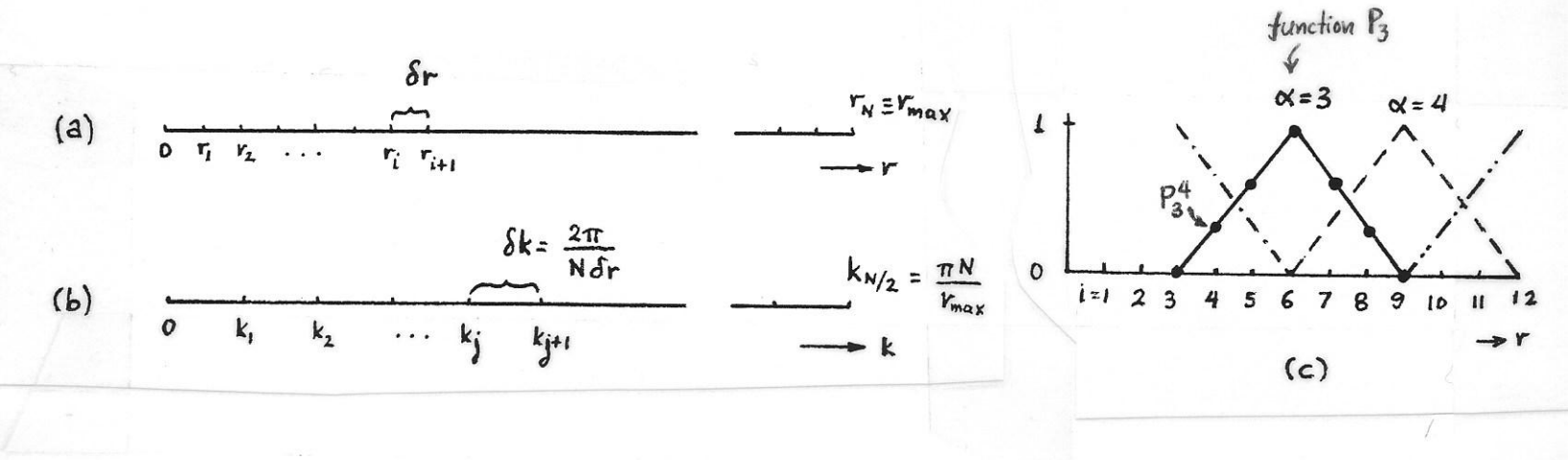

Figure 9.13 (a) Discretization of the r- axis employed in the numerical solution of an integral equation theory. (b) Discretization of the k- axis employed for calculations in Fourier-transformed space. (c) "Roof"-type basis functions P_α employed frequently in Gillan's method. The basis functions for $\alpha = 3$ and $\alpha = 4$ are shown, along with parts of the functions $\alpha = 2$ and $\alpha = 5$. P_α^i stands for the value of basis function P_α at grid point i on the r-axis.

h can be obtained from **c** via the closure relations, and vice versa. Thus, either **h** or **c** can be considered as the vector of unknowns of the numerical problem. In practice, the difference function $\gamma = \mathbf{h} - \mathbf{c}$ is a better choice as the vector of unknowns, as $\gamma(r)$ exhibits a smoother dependence on r than either h or c.

Upon incorporation of the closure relation between h and c, the Ornstein-Zernike equation,

$$h(r) - c(r) = \rho \int d^3r'\, h(\mathbf{r}')\, c(|\mathbf{r} - \mathbf{r}'|)$$

is converted into a set of nonlinear algebraic equations in γ. In practice, it is much more efficient to use the OZ equation in Fourier space,

$$\hat{h}(\mathbf{k}) = \hat{c}(\mathbf{k}) + \rho\, \hat{h}(\mathbf{k})\, \hat{c}(\mathbf{k})$$

For the numerical representation of the Fourier transformed correlation functions, k-space is discretized into equal intervals of width $\delta k = \dfrac{2\,\pi}{N\,\delta r}$) (see Fig. 9.13($b$). The vector $\hat{\mathbf{h}}$ of values of the Fourier transformed function $\hat{h}(k)$ can be obtained from $\mathbf{h}$ through a *Fast Fourier Transform* (FFT) calculation involving only $O(N \log_2 N)$ operations; the FFT algorithm can also be used inversely to form $\mathbf{h}$ from $\hat{\mathbf{h}}$. Similarly, $\hat{\mathbf{c}}$ can be obtained from $\mathbf{c}$ through an FFT, and vice versa.

A simple numerical scheme for solving the set of nonlinear algebraic equations obtained by discretizing the integral equation theory is successive substitution (*Picard scheme*). This scheme proceeds as follows:

(i) Guess γ

(ii) Find $\mathbf{c}$ from γ through the closure equation. For example, if the PY closure is invoked, one uses

$$c_i = (1 + \gamma_i)\, [\exp(-\beta \mathcal{V}_{pair,i}) - 1]$$

(*iii*) Find $\hat{\mathbf{c}}$ from $\mathbf{c}$ through an FFT calculation:

$$\hat{c}_j \equiv \hat{c}(k_j) = \frac{4\,\pi\,\delta r}{k_j} \sum_{i=1}^{N/2-1} r_i\,\sin(k_j\,r_j)\,c_i \quad , \quad k_j = \frac{2\pi\,j}{N\,\delta r}$$

(*iv*) Find $\hat{\gamma}$ from $\hat{\mathbf{c}}$ by invoking the Ornstein-Zernike equation:

$$\hat{\gamma}_j = \rho \frac{\hat{c}_j^2}{1 - \rho\,\hat{c}_j}$$

(*v*) Determine an updated estimate γ' as the inverse Fourier transform of γ, through FFT:

$$\gamma_i' = \frac{\delta k}{2\pi^2\,r_i} \sum_{j=1}^{N/2-1} k_j\,\sin(k_j\,r_j)\,\hat{\gamma}_j$$

(*vi*) Return to step (*ii*) and iterate, until two successive estimates of γ are closer to each other than a prespecified tolerance.

The Picard successive substitution scheme defined by the above algorithm is very inefficient; it leads to convergence only at low densities and high temperatures, and if one starts from an initial guess close to the solution. "Mixing" of successive approximations to γ may be used to prevent divergence. Even then, hundreds to thousands of iterations may be needed to achieve convergence at liquid densities, even with a good initial guess [Hansen and McDonald (1986)].

A better scheme for the numerical solution of the system of nonlinear algebraic equations obtained from the integral equation theory would be *Newton- Raphson* iteration with respect to γ. This scheme is quadratically convergent sufficiently close to the solution [Press *et al.* (1986)]. A problem with Newton-Raphson iteration with respect to the function values at all grid points is that a $N \times N$ Jacobian matrix has to be inverted

at each iteration; for N on the order of 1024, this $O(N^3)$ calculation is formidable with conventional hardware, although doable on present-day pipeline and parallel machines.

M.J. Gillan devised a compromise between the successive substitution and Newton-Raphson methods that is very efficient for solving integral equations. Gillan's method is based upon decomposing γ into a *coarse* and a *fine* part [Gillan (1979)]. A change in the coarse part of γ affects its overall shape or magnitude, while changes in the fine part occur over length scales much smaller than the scale characterizing the exact solution for γ, or only affect the tail of γ at large r (see Fig. 9.14)

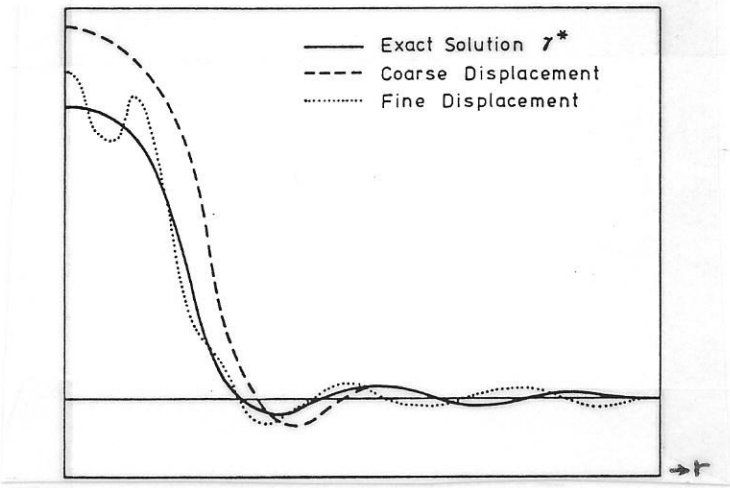

Figure 9.14 Illustration of the qualitative distinction between the coarse and the fine part of γ employed in Gillan's method. [Gillan (1979)].

A set of basis functions $\{P_\alpha\}$, $\alpha = 1, 2, \ldots, \nu$ with $\nu < N$ is introduced for expressing the coarse part of γ. The basis functions $\{P_\alpha\}$ span the entire r-domain over which $\gamma(r)$ has to be calculated. A convenient choice for $\{P_\alpha\}$ as piecewise linear functions, frequently referred to as "roof functions", is shown schematically in Figure 9.13(c). The symbol P_α^i will be used to denote the value of function P_α at grid point i on the r-axis. Note that, in the example of Figure 9.13(c), each P_α is nonzero at 5 node points. Note

also that the number ν of basis functions in this example is smaller than the number of grid points N by roughly a factor of 3. The decomposition of γ is implemented as follows:

$$\gamma_i = \sum_\alpha a_\alpha P_\alpha^i + \Delta\gamma_i$$

where the sum over α constitutes the coarse part, and $\Delta\gamma_i$ is the fine part at grid point i. The values $\Delta\gamma_i$ are chosen so as to satisfy

$$\sum_i P_\alpha^i \Delta\gamma_i = 0 \quad \text{for every } \alpha = 1, 2, \ldots, \nu$$

Determining the coarse part coefficients a_α and the fine part contributions $\Delta\gamma_i$ given a set of values for $\{\gamma_i\}$ amounts to solving a system of linear equations, and can be accomplished very fast [Gillan (1979)]. Gillan's method employs two kinds of iterations to determine a_α and $\Delta\gamma_i$:

- Iteration with the *Newton-Raphson* method under fixed fine part $\{\Delta\gamma_i\}$ to determine the coefficients $\{a_\alpha\}$ so that the OZ equations are satisfied. Note that only a $\nu \times \nu$ Jacobian matrix has to be inverted in each such iteration, which represents a drastic savings relative to the full-blown $N \times N$ Newton-Raphson scheme. The Jacobian matrix required in these Newton-Raphson iterations is readily calculable by passing into the Fourier-transformed domain [Gillan (1979)].
- Iteration with the *Picard method* to determine the fine part $\{\Delta\gamma_i\}$ so that the OZ equations are satisfied; The coefficients $\{a_\alpha\}$ and, therefore, the coarse part remain unchanged during a Picard iteration.

A flow diagram of the computations involved in Gillan's method is given in Figure 9.15. The iterations are carried out until both the coarse and the fine part have

converged up to a prespecified tolerance. Using this scheme, it is possible to arrive at well-converged solutions in 20 to 30 iterations. The method is quite robust with respect to the initial guess used for γ.

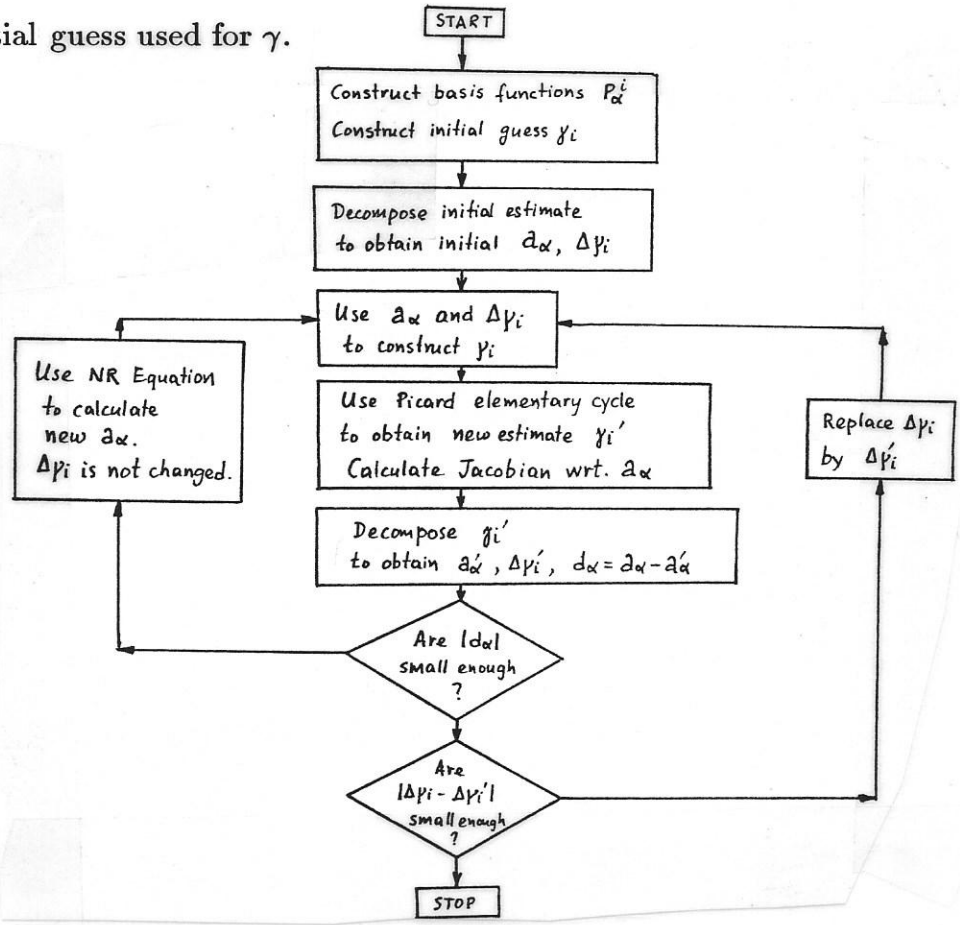

Figure 9.15 Flow diagram of computations involved in Gillan's method for the solution of integral equations for liquid structure. [adapted from Gillan (1979)].

9.3 Elements of Perturbation Theory

In most physical systems, the pair potentt gives rise to forces between molecules or interaction sites can be separated into a harsh, short-range repulsive part that rises very steeply with decreasing distance and a smoothly varying attractive part that tails off

gradually with increasing distance. As we saw in Section 5.3, J.D. van der Waals introduced the important idea that the structure of a homogeneous fluid away from the critical point is largely determined by geometric factors associated with packing of the repulsive cores of molecules. Attractive interactions may, in a first approximation, be regarded as giving rise to a uniform background potential that provides the cohesive energy of the fluid but has little effect on its structure.

This idea suggests that the structure and properties of a liquid could be related to those of a *reference system* characterized by a purely repulsive potential, *the attractive part of the potential being treated as a perturbation.* Accomplishing this task is the objective of perturbation theories for liquids. In a perturbation theory, the pair potential $\mathcal{V}_{pair}(r)$ is separated into a reference system part $v_0(r)$ and a perturbation part $w(r)$:

$$\mathcal{V}_{pair}(r) = v_0(r) + w(r) \tag{9.64}$$

Figure 9.15 shows three separations of the Lennard- Jones potential that have been used for constructing perturbation theories for liquids. In each case, the repulsive pair potential $v_0(r)$ of the reference fluid is represented as a solid line, while the attractive perturbation $w(r)$ is shown as a dotted line. Separation (a) defines $v_0(r)$ and $w(r)$ as the r^{-6} and r^{-12} terms in the LJ potential, respectively. Separation (b) employs the full LJ for $r < \sigma$ as the reference potential, treating the full potential for $r > \sigma$ as a perturbation. Separation (c) clips the LJ pair potential curve at its minimum and raises the part corresponding to $r < \sigma\, 2^{1/6}$ by ϵ to define the reference $v_0(r)$; as a result, $w(r)$ equals $-\epsilon$ for $0 < r < \sigma\, 2^{1/6}$ and the full LJ potential for $r > \sigma\, 2^{1/6}$. Of these three separations, (c) has the advantage that $w(r)$ is a slowly varying function of r throughout its domain,

and hence a first-order perturbation scheme is sufficient for describing its consequences on properties.

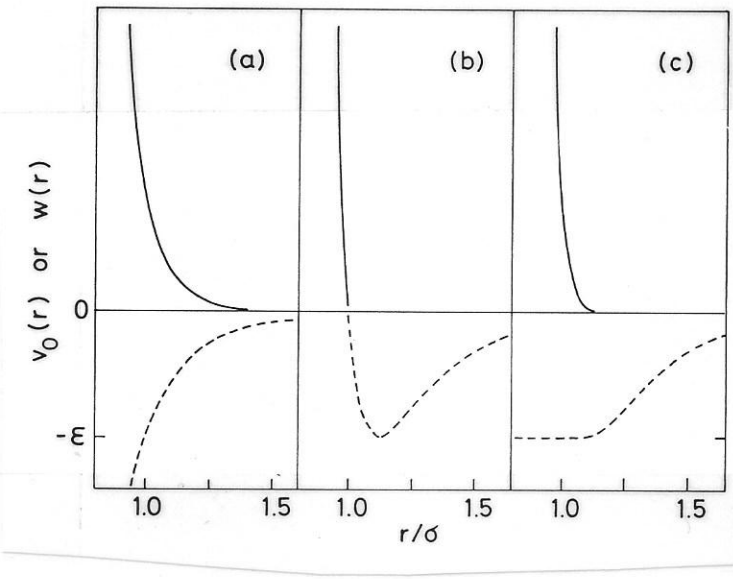

Figure 9.15 Three separations of the Lennard-Jones potential that have been used in perturbation theories: (a) Mc Quarrie and Katz (1966); (*b*) Barker and Henderson (1967); (*c*) Weeks, Chandler, and Andersen (1971) [after Hansen and McDonald (1986)].

The structure and thermodynamics of fluids characterized by "soft" repulsive core pair potentials, such as the $v_0(r)$ potentials shown in Figure 9.15, are not known analytically. On the contrary, as we have seen in section 9.2.3, accurate analytic expressions exist for the structure and thermodynamic properties of the hard-sphere fluid. Thus, in dealing with the reference fluid governed by $v_0(r)$, about which the perturbation $w(r)$ is made, an additional useful approximation is to define an *equivalent hard sphere system.* This hard sphere system is characterized by an appropriately chosen hard-sphere diameter d, such that its structure is as close as possible to that of the reference, soft repulsive core, system. Analytic perturbation theories for fluids with continuous potentials,

therefore, typically entail two levels of approximation. One deals with the problem of expressing the thermodynamics of the actual fluid in terms of the structure of a reference fluid with a soft repulsive pair potential, the attractive part of the actual potential being treated as a perturbation. A second level of approximation deals with mapping the structure of the soft core reference fluid onto that of a hard repulsive core system.

Our discussion in this chapter starts with some perfectly general strategies for expressing the Helmholtz energy of a system in terms of averages calculated with respect to the canonical ensemble probability density of a system with a different Hamiltonian (section 9.3.1). We show that these strategies can form a basis for expressing the Helmholtz energy as a perturbation expansion around the Helmholtz energy of a reference system whose statistical mechanics is known (section 9.3.2). By specializing to a fluid with pairwise additive forces, we show that the separation, Eq. (9.64), can be used to derive thermodynamic properties if the distribution functions characterizing the structure of the reference fluid are known (sections 9.3.2 and 9.3.3). Finally, we discuss a particular example of perturbation theory for the LJ fluid, showing how the soft repulsive core reference can be substituted by an equivalent system of hard spheres (section 9.3.4).

9.3.1 Free energy difference from a reference system expressed as an ensemble average in the reference system

Consider two classical systems, governed by the Hamiltonians $\mathcal{H}_0(\mathbf{r},\mathbf{p})$ and $\mathcal{H}(\mathbf{r},\mathbf{p})$. We assume that we are able to calculate the thermodynamic properties of system 0 (the *reference system*). In particular, we can readily obtain the Helmholtz energy function

$A_0(N,V,T)$ for that system. The direct calculation of thermodynamic properties for the other *perturbed* system poses mathematical difficulties. Thus, we are thinking of expressing these properties in a manner that takes advantage of our knowledge of the reference system. In particular, we are thinking of expressing the Helmholtz energy difference between the two systems at the same temperature and density, $A(N,V,T) - A_0(N,V,T)$, as an ensemble average in system 0. By definition,

$$A(N,V,T) - A_0(N,V,T) = -k_B T \ln \frac{Q(N,V,T)}{Q_0(N,V,T)} =$$

$$-k_B T \ln \frac{\int \exp\left[-\beta \mathcal{H}(\mathbf{p},\mathbf{r})\right] \; d^{3N}r \, d^{3N}p}{\int \exp\left[-\beta \mathcal{H}_0(\mathbf{p},\mathbf{r})\right] \; d^{3N}r \, d^{3N}p} =$$

$$-k_B T \ln \frac{\int \exp\left[-\beta \mathcal{H}_0(\mathbf{p},\mathbf{r})\right] \; \exp\left[-\beta \left\{\mathcal{H}(\mathbf{p},\mathbf{r}) - \mathcal{H}_0(\mathbf{p},\mathbf{r})\right\}\right] \; d^{3N}r \, d^{3N}p}{\int \exp\left[-\beta \mathcal{H}_0(\mathbf{p},\mathbf{r})\right] \; d^{3N}r \, d^{3N}p} \quad , \quad or$$

$$A(N,V,T) - A_0(N,V,T) = -k_B T \ln \left\langle \exp\left\{-\beta \left[\mathcal{H}(\mathbf{p},\mathbf{r}) - \mathcal{H}_0(\mathbf{p},\mathbf{r})\right]\right\}\right\rangle_0 \qquad (9.65)$$

where the angular brackets denote a phase-space average in the reference system 0. Eq. (9.65) is an important result; as we shall see, it forms a basis for calculating free energy differences by molecular simulation.

If the molecular masses in the reference system and the system if interest are the same, the kinetic energy contributions to $\mathcal{H}$ and $\mathcal{H}_0$ are identical. Also, the integrations over momentum space in calculating $\langle \; \rangle_0$ cancel out, leading to the simpler result

$$A(N,V,T) - A_0(N,V,T) = -k_B T \ln \left\langle \exp\left\{-\beta \left[\mathcal{V}(\mathbf{p},\mathbf{r}) - \mathcal{V}_0(\mathbf{p},\mathbf{r}]\right\}\right\rangle_0 \qquad (9.66)$$

In Eq. (9.66), the angular brackets denote a configuration-space average over the reference system 0.

The reader will note that our derivation of the Widom test particle insertion expression, Eq. (4.74), is a special case of Eq. (9.66). Both reference and perturbed systems in that case contained $(N+1)$ molecules. (Reference system: N "real" molecules interacting with each other, and 1 "phantom" molecule moving in the same volume; perturbed system: $(N+1)$ "real" molecules interacting with each other).

A simpler analogue of Eq. (9.66) is obtained when the system of interest differs only infinitesimally from the reference system. Consider a class of systems with potential energy function $\mathcal{V}(\lambda;\mathbf{r}) \equiv \mathcal{V}(\lambda)$, where λ is a *parameter*. As λ is changed away from the value λ_0 of the reference system, the interactions change, and the system gradually "mutates" into a system with different thermodynamic properties. At a given value of λ,

$$A(\lambda;\, N,V,T) \equiv A(\lambda) = -k_BT\, \ln Q(\lambda,\, N,V,T) =$$

$$-k_BT \ln \left[\frac{1}{N!\,\Lambda^{3N}} \int \exp\left[-\beta \mathcal{V}(\lambda;\, \mathbf{r})\right]\, d^{3N}r \right]$$

Assuming that changes in λ do not affect the molecular masses,

$$\frac{\partial A(\lambda;\, N,V,T)}{\partial \lambda} = -k_BT \frac{-\beta \int \exp\left[-\beta \mathcal{V}(\lambda;\, \mathbf{r})\right]\, \dfrac{\partial \mathcal{V}(\lambda;\, \mathbf{r})}{\partial \lambda}\, d^{3N}r}{\int \exp\left[-\beta \mathcal{V}(\lambda;\, \mathbf{r})\right]\, d^{3N}r} = \left\langle \frac{\partial \mathcal{V}(\lambda;\, \mathbf{r})}{\partial \lambda} \right\rangle_\lambda$$

Integrating,

$$A(\lambda_1) = A(\lambda_0) + \int_{\lambda_0}^{\lambda_1} \left\langle \frac{\partial \mathcal{V}(\lambda;\, \mathbf{r})}{\partial \lambda} \right\rangle_\lambda d\lambda \equiv A_0 + \int_{\lambda_0}^{\lambda_1} \langle \mathcal{V}'(\lambda) \rangle_\lambda \, d\lambda \qquad (9.67)$$

where the symbolism $\langle\ \rangle_\lambda$ indicates a canonical ensemble average over all configuration space, with the probability density evaluated at parameter value λ. Note that, in Eqs. (9.66) and (9.67), the A's can be identified with the *excess* Helmholtz energies, as the ideal gas contribution to A is the same in both reference and perturbed systems.

9.3.2 The λ- expansion and the high-temperature expansion for the excess free energy of a fluid

Eq. (9.67) is exact but not entirely convenient, because the average $\langle \mathcal{V}'(\lambda) \rangle_\lambda$ appearing in the integral is evaluated over an ensemble governed by a parameter value λ intermediate between the reference system value λ_0 and the value λ_1 of the system of interest. It would be more useful to express A in terms of ensemble averages evaluated at $\lambda = \lambda_0$, *i.e.*, at the parameter value characteristic of the reference system, whose properties we know. To accomplish this, we attempt a Taylor expansion of $\langle \mathcal{V}'(\lambda) \rangle_\lambda$ in powers of λ around $\lambda = \lambda_0$:

$$\langle \mathcal{V}'(\lambda) \rangle_\lambda = \{ \langle \mathcal{V}'(\lambda) \rangle_\lambda \}_{\lambda=\lambda_0} + (\lambda - \lambda_0) \left(\frac{\partial}{\partial \lambda} \langle \mathcal{V}'(\lambda) \rangle_\lambda \right)_{\lambda=\lambda_0} + \mathcal{O}(\lambda - \lambda_0)^2$$

But

$$\frac{\partial}{\partial \lambda} \langle \mathcal{V}'(\lambda) \rangle_\lambda = \frac{\partial}{\partial \lambda} \frac{\int \exp\left[-\beta \mathcal{V}(\lambda)\right] \mathcal{V}'(\lambda)\, d^{3N}r}{\int \exp\left[-\beta \mathcal{V}(\lambda)\right] d^{3N}r} =$$

$$\frac{\dfrac{\partial}{\partial \lambda} \displaystyle\int \exp\left[-\beta \mathcal{V}(\lambda)\right] \mathcal{V}'(\lambda)\, d^{3N}r}{\displaystyle\int \exp\left[-\beta \mathcal{V}(\lambda)\right] d^{3N}r} -$$

$$\frac{\left\{ \displaystyle\int \exp\left[-\beta \mathcal{V}(\lambda)\right] \mathcal{V}'(\lambda)\, d^{3N}r \right\} \dfrac{\partial}{\partial \lambda} \displaystyle\int \exp\left[-\beta \mathcal{V}(\lambda)\right] d^{3N}r}{\left[\displaystyle\int \exp\left[-\beta \mathcal{V}(\lambda)\right] d^{3N}r \right]^2} =$$

$$\frac{-\beta \int \exp\left[-\beta \mathcal{V}(\lambda)\right] \left[\mathcal{V}'(\lambda)\right]^2 d^{3N}r}{\int \exp\left[-\beta \mathcal{V}(\lambda)\right] d^{3N}r} + \frac{\int \exp\left[-\beta \mathcal{V}(\lambda)\right] \mathcal{V}''(\lambda)\, d^{3N}r}{\int \exp\left[-\beta \mathcal{V}(\lambda)\right] d^{3N}r} +$$

$$\beta \left\{ \frac{\int \exp\left[-\beta \mathcal{V}(\lambda)\right] \mathcal{V}'(\lambda)\, d^{3N}r}{\int \exp\left[-\beta \mathcal{V}(\lambda)\right] d^{3N}r} \right\}^2 = -\beta \left\langle \left[\mathcal{V}'(\lambda)\right]^2 \right\rangle_\lambda + \langle \mathcal{V}''(\lambda) \rangle_\lambda + \beta \left[\langle \mathcal{V}'(\lambda) \rangle_\lambda \right]^2$$

Hence,

$$\langle \mathcal{V}'(\lambda) \rangle_\lambda = \{ \langle \mathcal{V}'(\lambda) \rangle \}_{\lambda=\lambda_0} +$$

$$(\lambda - \lambda_0)\left[\langle V''(\lambda)\rangle_\lambda - \beta\left(\left\langle [\mathcal{V}'(\lambda)]^2\right\rangle_\lambda - [\langle \mathcal{V}'(\lambda)\rangle_\lambda]^2\right)\right]_{\lambda=\lambda_0} + \mathcal{O}(\lambda - \lambda_0)^2$$

Introducing the short-hand notation

$$\{\langle f(\lambda)\rangle_\lambda\}_{\lambda=\lambda_0} \equiv \langle f(\lambda)\rangle_0$$

and substituting into Eq. (9.67), we obtain

$$\beta A(\lambda_1) = \beta A_0 + (\lambda_1 - \lambda_0)\beta\langle \mathcal{V}'(\lambda)\rangle_0 +$$

$$\frac{1}{2}(\lambda_1 - \lambda_0)^2\left\{\beta\langle \mathcal{V}''(\lambda)\rangle_0 - \beta^2\left[\left\langle [\mathcal{V}'(\lambda)]^2\right\rangle_0 - [\langle \mathcal{V}'(\lambda)\rangle_0]^2\right]\right\} + \mathcal{O}(\lambda_1 - \lambda_0)^3 \qquad (9.68)$$

We now specialize to the case of pairwise additive central interactions:

$$\mathcal{V}(\lambda) \equiv \mathcal{V}(\lambda; \mathbf{r}) = \sum_{i<}^{N}\sum_{j}^{N} v_\lambda(r_{ij})$$

where the pair potential is a *linear* function of the parameter λ:

$$v_\lambda(r) = v_0(r) + \lambda\, w(r) \quad (\lambda_0 = 0 < \lambda < \lambda_1 = 1) \qquad (9.64)$$

Defining the *total perturbation energy*

$$W = \sum_{i<}^{N}\sum_{j}^{N} w(r_{ij}) \qquad (9.69)$$

we obtain, from Eq. (9.68), the simpler equation

$$\beta A = \beta A_0 + \beta\langle W\rangle_0 - \frac{1}{2}\beta^2\left(\langle W^2\rangle_0 - \langle W\rangle_0^2\right) + \mathcal{O}(\beta^3) \qquad (9.70)$$

The series (9.70) is known as the *high-temperature expansion.* Note, however, that temperature appears not only in the powers of β, but also in the ensemble averages. The

coefficients of β in Eq. (9.70) are all *statistical averages evaluated in the reference-system ensemble*; that is, they can be evaluated if we know the statistical mechanics of the reference system.

Given the pairwise additive nature of the perturbation energy W [see Eq. (9.69)], and invoking Eq. (9.12) for the calculation of ensemble averages in the reference system, which is isotropic, we can write

$$\langle W \rangle_0 = \frac{N}{2} \rho \int g_0(r_{12})\, w(r_{12})\, d^3 r_{12} \tag{9.71}$$

Thus, to first order in β, the high temperature expansion of Eq. (9.71) gives

$$\beta \frac{A - A_0}{N} = \frac{1}{2} \beta \rho \int g_0(r_{12})\, w(r_{12})\, d^3 r_{12} \tag{9.72}$$

Expressions for the higher-order terms have been derived; they require knowledge of higher-order distribution functions of the reference system.

9.3.3 Gibbs- Bogoliubov Inequalities

An interesting double bound on A is provided by the Gibbs-Bogoliubov inequalities

$$\frac{\beta A_0}{N} + \frac{1}{2} \beta \rho \int g(r)\, w(r)\, d^3 r \leq \frac{\beta A}{N} \leq \frac{\beta A_0}{N} + \frac{1}{2} \beta \rho \int g_0(r)\, w(r)\, d^3 r \tag{9.73}$$

where $g_0(r)$ and $g(r)$ are the pair distribution functions describing the structure of the reference system and of the system of interest at density ρ and temperature T. The pair potential of the system of interest differs from that of the reference system by $w(r)$. Note that the right-hand side of the double inequality (9.73) informs us about the sign of the error committed by invoking the first order perturbation expansion, Eq. (9.72).

The double inequality (9.73) is essentially a consequence of Eq. (9.66) and the convexity of the exponential function. We present here a simple proof due to Isihara (1968) [Hansen and McDonald, 1986]:

Lemma

Let $\mathbf{F(r)}$, $\mathbf{G(r)}$ be two integrable, non-negative, but otherwise arbitrary configuration-space functions, defined such that

$$\int F(\mathbf{r})\, d^{3N}r = \int G(\mathbf{r})\, d^{3N}r \tag{9.74}$$

Then, the functions satisfy the inequality

$$\int F(\mathbf{r}) \ln F(\mathbf{r})\, d^{3N}r \geq \int F(\mathbf{r}) \ln G(\mathbf{r})\, d^{3N}r \tag{9.75}$$

Proof

The difference between left- and right- hand sides of Eq. (9.75) can be written as

$$\int F(\mathbf{r}) \ln F(\mathbf{r})\, d^{3N}r - \int F(\mathbf{r}) \ln G(\mathbf{r})\, d^{3N}r =$$

$$\int G(\mathbf{r}) \left[\frac{F(\mathbf{r})}{G(\mathbf{r})} \ln \left(\frac{F(\mathbf{r})}{G(\mathbf{r})} \right) - \frac{F(\mathbf{r})}{G(\mathbf{r})} + 1 \right] d^{3N}r$$

However as can readily be proved by considering the first derivative of the function $\ln x - 1 + \frac{1}{x}$,

$$x \ln x \geq x - 1 \quad \text{for every } x > 0$$

Hence,

$$\int G(\mathbf{r}) \left[\frac{F(\mathbf{r})}{G(\mathbf{r})} \ln \left(\frac{F(\mathbf{r})}{G(\mathbf{r})} \right) - \frac{F(\mathbf{r})}{G(\mathbf{r})} + 1 \right] d^{3N}r \geq 0 \quad , \quad \text{which gives}$$

$$\int F(\mathbf{r}) \ln F(\mathbf{r})\, d^{3N}r \geq \int F(\mathbf{r}) \ln G(\mathbf{r})\, d^{3N}r \quad \text{Q.E.D.}$$

To prove the Gibbs-Bogoliubov double inequality, we apply Eq. (9.75) with

$$F(\mathbf{r}) = \exp\left[\beta\left(A_0 - \mathcal{V}_0(\mathbf{r})\right)\right] = \frac{\exp\left(-\beta\mathcal{V}_0(\mathbf{r})\right)}{Z_0}$$

$$G(\mathbf{r}) = \exp\left[\beta\left(A - \mathcal{V}(\mathbf{r})\right)\right] = \frac{\exp\left(-\beta\mathcal{V}(\mathbf{r})\right)}{Z}$$

By definition, $F(\mathbf{r})$ and $G(\mathbf{r})$ are the canonical ensemble configurational probability densities for the reference system and the perturbed system. Both are normalized, and therefore satisfy Eq. (9.74). By the above lemma we obtain

$$\langle A_0 - \mathcal{V}_0(\mathbf{r})\rangle_0 \geq \langle A - \mathcal{V}(\mathbf{r})\rangle_0 \quad \text{or} \quad A \leq A_0 + \langle \mathcal{V}(\mathbf{r}) - \mathcal{V}_0(\mathbf{r})\rangle_0 \tag{9.76}$$

On the other hand, applying Eq. (9.75) with

$$F(\mathbf{r}) = \exp\left[\beta\left(A - \mathcal{V}(\mathbf{r})\right)\right]$$

$$G(\mathbf{r}) = \exp\left[\beta\left(A_0 - \mathcal{V}_0(\mathbf{r})\right)\right]$$

we obtain

$$\langle A - \mathcal{V}(\mathbf{r})\rangle \geq \langle A_0 - \mathcal{V}_0(\mathbf{r})\rangle \quad \text{or} \quad A \geq A_0 + \langle \mathcal{V}(\mathbf{r}) - \mathcal{V}_0(\mathbf{r})\rangle \tag{9.77}$$

Combining Eqs. (9.76) and (9.77), one obtains

$$A_0 + \langle \mathcal{V}(\mathbf{r}) - \mathcal{V}_0(\mathbf{r})\rangle \leq A \leq A_0 + \langle \mathcal{V}(\mathbf{r}) - \mathcal{V}_0(\mathbf{r})\rangle_0 \tag{9.78}$$

In the case where the potential energy functions $\mathcal{V}$, $\mathcal{V}_0$ are of the form of Eq. (9.64) with $\lambda = 1$, Eq. (9.78) reduces to

$$A_0 + \left\langle \sum_{i<j}^{N} \sum^{N} w(r) \right\rangle \leq A \leq A_0 + \left\langle \sum_{i<j}^{N} \sum^{N} w(r) \right\rangle_0$$

or, in view of Eq. (9.12),

$$A_0 + \frac{1}{2} N\rho \int g(r) w(r)\, d^3 r \leq A \leq A_0 + \frac{1}{2} N\rho \int g_0(r) w(r)\, d^3 r \tag{9.73}$$

which is the Gibbs-Bogoliubov inrquality.

The right-hand side of the double inequality, Eq. (9.73), is generally more useful that the left, as it invokes the structure of the reference fluid, which is known. This right-hand side of (9.73) can form the basis for a *variational approach* to liquid theory, as follows:

- Given the system of interest (*e.g.*, LJ fluid), choose a reference fluid (*e.g.*, hard sphere fluid), whose potential depends on one or more parameters (*e.g.*, the hard-sphere diameter).
- For given density and temperature, determine the minimum value of $A_0 + \frac{1}{2} N\rho \int g_0(r) w(r)\, d^3 r$ with respect to the potential parameters of the reference fluid.
- Use the resulting minimum as an estimate for $A(\rho, T)$ of the system of interest under the considered density and temperature.

For the LJ fluid, this variational approach gives results within 5 % of the exact results obtained from simulation.

9.3.4 A note on Chandler - Weeks - Andersen perturbation theory: Application to the Lennard-Jones fluid

As already mentioned in conjunction with Fig. 9.15(c), the perturbation theory of Chandler - Weeks - Andersen employs the following separation of the LJ pair potential [Weeks *et al.* (1971)]:

$$\mathcal{V}_{pair}(r) = u_0(r) + w(r) \tag{9.79}$$

where

$$u_0(r) = \begin{cases} \mathcal{V}(r) + \epsilon & \text{if } r < 2^{1/6}\,\sigma \\ 0 & \text{if } r \geq 2^{1/6}\,\sigma \end{cases}$$

$$w(r) = \begin{cases} -\epsilon & \text{if } r < 2^{1/6}\,\sigma \\ \mathcal{V}_{pair}(r) & \text{if } r \geq 2^{1/6}\,\sigma \end{cases}$$

In contrast to other separations, the CWA separation results in a smoothly varying $w(r)$ in the region of the minimum, so that a first-order perturbation expansion of the type of Eq. (9.72) suffices for the treatment of attractive forces. For implementing Eq. (9.72), one needs the structure ($g_0(r)$) of the reference system. An analytical solution for the statistical mechanics of a fluid characterized by the soft repulsive core potential $u_0(r)$ is not available, however. Thus, one is led to the problem of approximating the reference system by an equivalent hard sphere system, for which an analytic solution is available (see section 9.2.3). More specifically, one needs to choose an appropriate *hard sphere system*, of sphere diameter d, whose structure provides a good approximation for $g_0(r)$. The desired pair distribution function of the reference system will be expressed as

$$g_0(r) \simeq y_d(r)\, exp\,[-\beta\, u_0(r)] \tag{9.80}$$

where $y_d(r)$ is the y- correlation function characterizing the equivalent hard sphere fluid. As pointed out in section 9.2.2, this is a continuous function that remains relatively insensitive to the exact form of the potential.

The problem of defining an equivalent hard sphere system has been reduced to the question: What is the best way to choose an equivalent hard-sphere diameter d for approximating the structure of the reference fluid by Eq. (9.80) at given density and temperature?

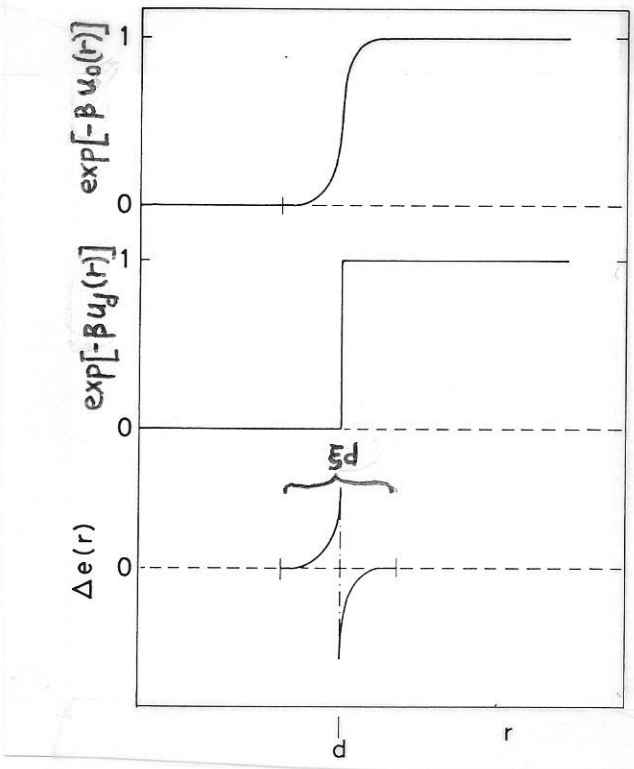

Figure 9.16 The "blip function", involved in defining an equivalent hard sphere diameter for a soft repulsive potential in the perturbation theory of Chandler, Weeks, and Andersen [Andersen, Weeks, and Chandler (1971)].

The analysis of Andersen, Weeks, and Chandler (1971) pointed to the following function as useful for addressing the problem of choosing an equivalent hard-sphere diameter:

$$\Delta e(r) \equiv \exp\left[-\beta\, u_0(r)\right] - \exp\left[-\beta\, u_d(r)\right] \tag{9.81}$$

A sketch of $\exp\left[-\beta\, u_0(r)\right]$, $\exp\left[-\beta\, u_d(r)\right]$, and $\Delta e(r)$ is given in Fig. 9.16.

The Boltzmann factor $\exp\left[-\beta u_0(r)\right]$ of the soft repulsive core potential rises from 0 to 1 over a steep section of sigmoidal shape. The function $\exp\left[-\beta\, u_d(r)\right]$ is a Heaviside step function at $r = d$. The difference function $\Delta e(r)$ is nonzero only over a narrow range of width $\xi\, d$ around $r = d$ ("blip function").

A functional Taylor expansion of the Helmholtz energy density of the soft-core reference system in powers of $\Delta e(r)$ leads to

$$\frac{\beta A}{V} = \frac{\beta A_d}{V} - \frac{1}{2}\rho^2 \int y_d(r)\, \Delta e(r)\, d^3 r + \mathcal{O}(\xi^4) \tag{9.82}$$

where A_d is the Helmholtz energy of the hard sphere fluid. [Hansen and McDonald (1986)].

In view of Eq. (9.82), Andersen, Weeks, and Chandler determined the optimal equivalent hard sphere diameter to match the soft repulsive core reference system by imposing the condition

$$\int y_d(r)\, \Delta e(r)\, d^3 r = 0 \quad \text{or, more explicitly,}$$

$$\int y_d(r)\, \left\{\exp\left[-\beta\, u_0(r)\right] - \exp\left[-\beta\, u_d(r)\right]\right\}\, d^3 r = 0 \tag{9.83}$$

The function $y_d(r)$ is known analytically from the Percus-Yevick approximate solution for hard spheres, Eq. (9.59). In practice, empirical expressions that bring $y_d(r)$ very close to the exact hard sphere simulation results can be used in place of the PY solution [Verlet and Weis (1972)]. Eq. (9.83) is an implicit equation in the hard-sphere diameter d, from which the hard-sphere system equivalent to the soft repulsive reference potential $u_0(r)$ can be determined.

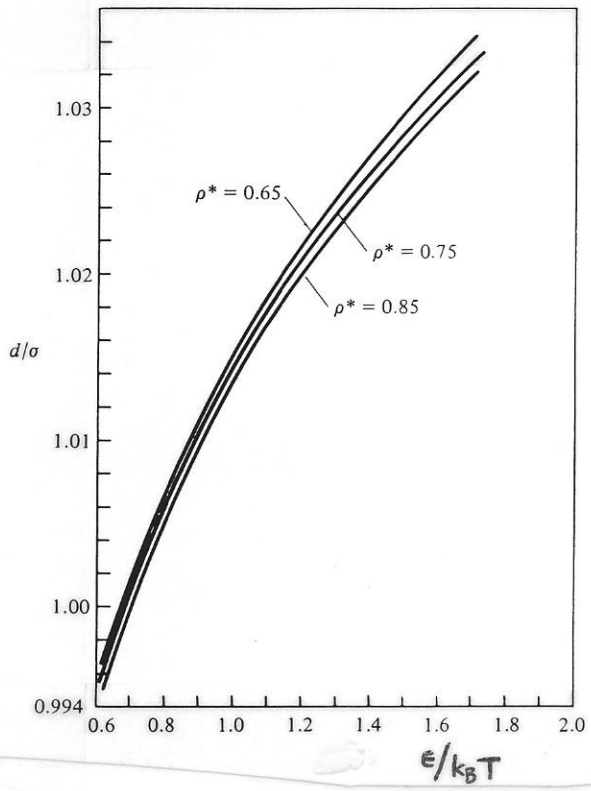

Figure 9.17 Equivalent hard sphere diameter for the reference fluid used in the Chandler-Weeks- Andersen perturbation theory for the Lennard-Jones fluid. The hard sphere diameter d is a function of both temperature and density. σ and ϵ are the LJ potential parameters [after McQuarrie (1979)].

An interesting observation is that, with the approximation (9.80) for $g_0(r)$, Eq. (9.83) can be written equivalently as

$$\int \{y_d(r) \exp[-\beta u_0(r)] - 1\}\, d^3r = \int \{y_d(r) \exp[-\beta u_d(r)] - 1\}\, d^3r \quad \text{or}$$

$$\int [g_0(r) - 1]\, d^3r = \int [g_d(r) - 1]\, d^3r$$

Invoking Eq. (9.35), the last relation can be written

$$\kappa_{T,0} = \kappa_{T,d}$$

One can therefore say that the CWA prescription defines the equivalent hard sphere diameter in such a way as to match the isothermal compressibility of the soft core reference fluid with that of the equivalent hard sphere fluid.

Clearly, the equivalent hard-sphere diameter determined from Eq. (9.83) is a function of *temperature and density.* In general, d decreases considerably with increasing temperature; it also decreases somewhat with increasing density (see Figure 9.17).

Having obtained an approximate structure $g_0(r)$ for the reference system via Eq. (9.80), one can obtain the thermodynamics of the LJ system from the high- temperature expansion truncated at the first term. From Eq. (9.72) we obtain:

Excess Helmholtz energy

$$\frac{\beta A^{ex}}{N} = \frac{\beta A_0^{ex}}{N} + \frac{1}{2}\beta\rho \int g_0(r)\, w(r)\, d^{3N}r \tag{9.72}$$

All thermodynamic properties can be obtained from the temperature- and density dependence of A^{ex}. In practice, the following approximations are frequently used:

Pressure [compare Eq. (9.34)]

$$\frac{\beta P}{\rho} = 1 - \frac{1}{6}\beta\rho \int r \left(\frac{\partial u_0}{\partial r} + \frac{\partial w}{\partial r} \right) g_0(r)\, d^3 r \tag{9.84}$$

Excess energy

$$\frac{U^{ex}}{N} = \frac{1}{2}\rho \int (u_0 + w)\, g_0(r)\, d^3 r \tag{9.85}$$

The CWA perturbation scheme leads to results that are in favorable agreement with simulation data for the LJ fluid over a wide range of conditions.

Table 9.1

Pressure and excess energy for the LJ Fluid estimated with the CWA scheme at a density of $\rho\sigma^3 = 0.85$.

Exact results obtained via MD simulation are also listed, along with results from applying the PY closure directly to the full 6-12 potential

	$\frac{\beta P}{\rho}$, Eq. (9.84)			$\frac{-\beta U^{ex}}{N}$, Eq. (9.85)		
$\frac{k_B T}{\epsilon}$	CWA	MD	PY	CWA	MD	PY
1.128	2.82	2.78	3.57	5.08	5.05	4.98
0.880	1.82	1.64	3.17	6.77	6.75	6.61
0.786	1.23	0.99	2.97	7.70	7.70	7.51
0.719	0.69	0.36	2.82	8.52	8.51	8.28

9.4 A Note on the Structure of Polymer Melts

9.4.1 Intermolecular and Intramolecular Parts of the Pair Distribution Function

In this section we briefly examine how the ideas introduced in the preceding sections of this chapter can be extended and applied to elucidate the structure and thermodynamics of a category of complex molecular systems of some technical significance, namely polymer melts.

For simplicity, we will confine our attention to linear polyethylene melts. The polymer chains will be modelled as sequences of skeletal methyl and methylene mers ("united atom representation"). Two skeletal units belonging to the same chain and separated by more than three bonds interact with each other via a LJ potential. The same potential is used between units belonging to different chains. Bond lengths and bond angles are kept fixed, and a torsional potential depending on the dihedral angle defined by four successive segments is used to describe the energetics of conformational isomerization. The potential parameters σ and ϵ describing methyl-methyl, methyl-methylene, and methylene-methylene interactions will be assumed identical. Thus, the model polyethylene system consists effectively of one type of interaction sites. In the following, the terms "mer" and "site" will be used interchangeably. The number of mers per chain will be denoted by n. Figure 9.18(a) shows how sites are connected along a chain. Note that the collision diameter σ of sites is much greater than the bond length; as a result, the repulsive core of a macromolecule can best be envisioned as a sequence of fused spheres.

In the melt, one can define a (total) site-site pair distribution function $g_{tot}(r)$ exactly as indicated in Fig. 9.1. If ρ is the density of sites (number of mers per unit volume of melt), $\rho\, g_{tot}(r)$ equals the local density of sites we expect to find at a distance r from a reference point at which we know that there is a site, averaged over all configurations. As shown in Fig. 9.18 (*b*), these sites may belong to the same chain as the reference site, or to other chains. Consequently, the total structure of the polymer melt can be separated into an intramolecular and an intermolecular part, as follows:

$$\rho g_{tot}(r) = \omega(r) + \rho\, g(r) \tag{9.86}$$

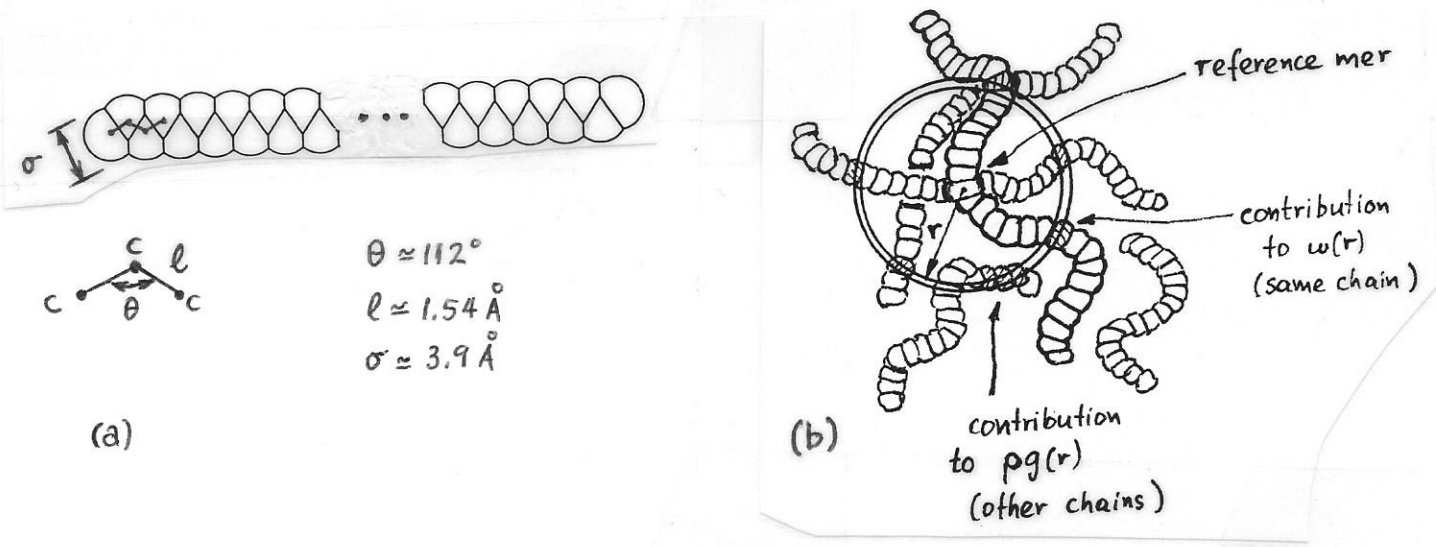

Figure 9.18 (*a*) Molecular geometry of polyethylene chain in the united atom representation. The chain is modelled as a sequence of methyl and methylene LJ sites. (*b*) Separation of the pair distribution function into an intermolecular and an intramolecular part.

$\omega(r)$ is the *intramolecular pair density function.* By definition, $\omega(r)$ is the local density of mers of a given chain at position $\mathbf{r}$, provided a mer of *the same* chain has been placed

at the origin, averaged over all configurations. Since chains are finite objects, we expect that

$$\lim_{r\to\infty} \omega(r) = 0$$

Also, by definition, the following normalization is obeyed:

$$\int_0^\infty 4\pi\, r^2\, \omega(r)\, dr = n - 1$$

$g(r)$ is the *intermolecular pair distribution function.* By definition, $\rho\, g(r)$ is the local density of mers belonging to *different* chains than the reference chain at position $\mathbf{r}$, provided a mer of the reference chain has been placed at the origin. At large distances, $g(r)$ exhibits a normalization behavior analogous to that of $g_{tot}(r)$:

$$\lim_{r\to\infty} g(r) = 1$$

9.4.2 Determination of the Chain Radius of Gyration in the Melt Through Small Angle Neutron Scattering

An interesting structural question with profound implications for thermodynamic, rheological, and mechanical behavior is, how do individual chains conform in the amorphous polymer bulk (polymer melts and amorphous polymer glasses)? Experimentally, this question was addressed in the early 1970s by small angle neutron scattering (SANS) measurements [Ballard *et al.* (1973), Kirste *et al.* (1973), Cotton *et al.* (1974)]. Here we discuss the principle of this measurement as an application of concepts introduced in sections 9.1.4 and 9.4.1.

The SANS measurement takes advantage of the very different coherent scattering cross-section of hydrogen and deuterium to generate contrast between individual chains and the surrounding polymer matrix without significantly perturbing interactions in the polymer system. A small number of isotopically "labelled" chains are dispersed in a matrix of unlabelled polymer. The labelled chains are identical to the matrix chains in architecture and molecular weight; their only difference is that they are made of carbon and deuterium, whereas the matrix chains are made of carbon and hydrogen (of vice versa). At high concentrations, the small difference in van der Waals interaction energy between labelled and unlabelled mers may lead to phase separation phenomena, but this does not constitute a problem in this measurement.

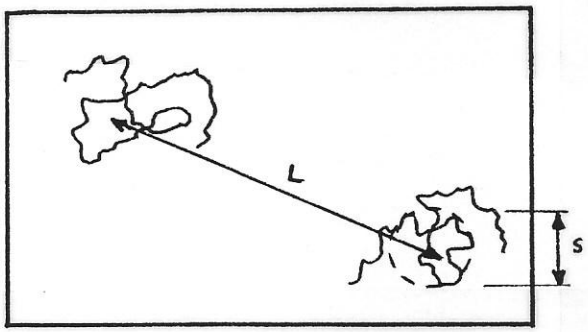

Figure 9.19 Schematic of deuterated polyethylene chains dispersed in a polyethylene melt matrix. The distance between chains, L, is much larger than the characteristic size of the polymer coils, s.

To analyze the information obtained from the SANS experiment, consider an infinitely dilute system of labelled chains in an unlabelled melt matrix (see Fig. 9.19).

The distances between labelled chains, L, are much larger than the length scale s characterizing the overall size of a polymer molecule. (A precise definition of s will be given soon.) The mers of labelled chains scatter neutrons. We wish to express the scattered intensity as a function of the scattering vector $\mathbf{k}$ in the small angle regime ($ks << 1$).

According to Eq. (9.29), the structure factor $S(k)$, $k \neq 0$ is related to the *total* pair distribution function $g_{tot}(r)$ between mers by

$$S(k) - 1 = \rho \int_0^\infty 4\pi r^2 \frac{\sin(kr)}{kr} [g_{tot}(r) - 1] \; dr \tag{9.87}$$

In writing Eq. (9.87), we have recognized that the system of labelled mers, which scatter the radiation, is isotropic. We have also recognized that the pair distribution function appearing in Eq. (9.29) describes *total* (rather than purely intermolecular) correlations in the macromolecular fluid.

As the labelled chains are infinitely dilute in the polymer matrix, the intermolecular pair distribution function describing correlations between their mers will be ideal gas-like. That is, one can write $g(r) \simeq 1$ for the intermolecular part of g_{tot}. Eq. (9.86) becomes

$$\rho \, g_{tot}(r) = \omega(r) + \rho \, g(r) \simeq \omega(r) + \rho \tag{9.88}$$

Combining Eqs. (9.87) and (9.88), we obtain

$$S(k) - 1 = \int_0^\infty 4\pi r^2 \frac{\sin(kr)}{kr} \omega(r) \, dr \equiv \hat{\omega}(k) = \frac{1}{n} \left\langle \sum_{\substack{i=1 \\ i \neq j}}^{n} \sum_{j=1}^{n} \frac{\sin(k \, r_{ij})}{k \, r_{ij}} \right\rangle \tag{9.89}$$

The ensemble average form on the right hand side of Eq. (9.89) is a direct consequence of the definition of $\omega(r)$. The transformation leading to this form is entirely analogous

to Eq. (9.12), with $\omega(r)$ playing the role of $\rho\, g(r)$ and n playing the role of N. The ensemble average is taken over the distribution of single-chain conformations adopted in the melt. Eq. (9.89) informs us that, in this infinitely dilute system of labelled chains, $S(k) - 1$ is the Fourier transform of the intramolecular pair density function. The structural information contained in the scattering pattern is purely intramolecular.

Specializing to the range where k is much smaller than the coil dimensions ($ks << 1$), we can simplify expression (9.89) for the structure factor. Recognizing that, for any pair of mers (i,j) on a chain, $k\,r_{ij} << 1$, we can approximate $\dfrac{\sin(k\,r_{ij})}{k\,r_{ij}}$ by the expansion

$$\frac{\sin(k\,r_{ij})}{k\,r_{ij}} = \frac{1}{k\,r_{ij}}\left[k\,r_{ij} - \frac{(k\,r_{ij})^3}{3!} + \frac{(k\,r_{ij})^5}{5!} - \cdots\right] =$$

$$1 - \frac{(k\,r_{ij})^2}{6} + \frac{(k\,r_{ij})^4}{120} + \cdots$$

Keeping terms up to second order in $k\,r_{ij}$, we obtain from Eq. (9.89):

$$S(k) - 1 \simeq \frac{1}{n}\left\langle \sum_{\substack{i=1 \\ i \neq j}}^{n} \sum_{j=1}^{n} \left\{1 - \frac{(k\,r_{ij})^2}{6}\right\} \right\rangle =$$

$$\frac{1}{n} \sum_{\substack{i=1 \\ i \neq j}}^{n} \sum_{j=1}^{n} 1 - \frac{1}{3n}\left\langle \sum_{\substack{i=1 \\ i < j}}^{n} \sum_{j=1}^{n} (k\,r_{ij})^2 \right\rangle =$$

$$\frac{n\,(n-1)}{n} - \frac{1}{3\,n}\left\langle \sum_{\substack{i=1 \\ i < j}}^{n} \sum_{j=1} (k\,r_{ij})^2 \right\rangle = n - 1 - \frac{k^2}{3\,n}\left\langle \sum_{1 \le i < j \le n} \sum r_{ij}^2 \right\rangle$$

Therefore, in the limit $ks << 1$, we can write

$$\text{"Debye scattering function"}\ P(k) = \frac{I(k)}{I(0)} = \frac{S(k)}{n} = 1 - \frac{k^2}{3}\frac{1}{n^2}\left\langle \sum_{1 \le i < j \le n} \sum r_{ij}^2 \right\rangle \qquad (9.90)$$

As is obvious from its derivation, Eq. (9.90) is not specific to a chain; it is valid for *any* finite body consisting of point scatterers, provided the scattering pattern is examined over a range of k^{-1} much larger than the overall dimensions of the body. The quantity $\frac{1}{n^2}\sum\sum_{1\le i<j\le n} r_{ij}^2$ is characteristic of the overall spatial distribution of points constituting the body. We attribute a concrete geometrical significance to this quantity by the following theorem:

Lagrange's theorem (1783)

Given a collection of n points of equal mass, located at positions $\mathbf{r}_i$, $1 \le i \le n$, the quantity $\frac{1}{n^2}\sum\sum_{1\le i<j\le n} r_{ij}^2$, where $r_{ij} \equiv |\mathbf{r}_j - \mathbf{r}_i|$, equals the *squared radius of gyration* s^2 of the collection of points.

Proof

By definition (cf. moment of inertia used to describe rigid body motion in mechanics), the radius of gyration s of a collection of material points of equal mass is

$$s^2 \equiv \frac{1}{n}\sum_{i=1}^{n}\left(\mathbf{r}_i - \frac{1}{n}\sum_{j=1}^{n}\mathbf{r}_j\right)^2 \tag{9.91}$$

Transforming Eq. (9.91),

$$s^2 = \frac{1}{n^3}\sum_{i=1}^{n}\left[n\,\mathbf{r}_i - \sum_{j=1}^{n}\mathbf{r}_j\right]^2 = \frac{1}{n^3}\sum_{i=1}^{n}\left[\sum_{j=1}^{n}(\mathbf{r}_i - \mathbf{r}_j)\right]^2 =$$

$$\frac{1}{n^3}\sum_{i=1}^{n}\left[\sum_{j=1}^{n}\sum_{k=1}^{n}(\mathbf{r}_i - \mathbf{r}_j)\cdot(\mathbf{r}_i - \mathbf{r}_k)\right]$$

Now, by the law of cosines,

$$(\mathbf{r}_i - \mathbf{r}_j)\cdot(\mathbf{r}_i - \mathbf{r}_k) = \frac{(\mathbf{r}_i - \mathbf{r}_j)^2 + (\mathbf{r}_i - \mathbf{r}_k)^2 - (\mathbf{r}_j - \mathbf{r}_k)^2}{2} \equiv \frac{r_{ij}^2 + r_{ik}^2 - r_{jk}^2}{2}$$

Substituting,

$$s^2 = \frac{1}{n^3}\sum_{i=1}^{n}\left[\sum_{j=1}^{n}\sum_{k=1}^{n}\frac{r_{ij}^2 + r_{ik}^2 - r_{jk}^2}{2}\right] =$$

$$\frac{1}{2n^3}\sum_{i=1}^{n}\sum_{j=1}^{n}\sum_{k=1}^{n} r_{ij}^2 + \frac{1}{2n^3}\sum_{i=1}^{n}\sum_{j=1}^{n}\sum_{k=1}^{n} r_{ik}^2 - \frac{1}{2n^3}\sum_{i=1}^{n}\sum_{j=1}^{n}\sum_{k=1}^{n} r_{jk}^2 =$$

$$\frac{1}{2n^2}\sum_{i=1}^{n}\sum_{j=1}^{n} r_{ij}^2 + \frac{1}{2n^2}\sum_{i=1}^{n}\sum_{k=1}^{n} r_{ik}^2 - \frac{1}{2n^3}\sum_{j=1}^{n}\sum_{k=1}^{n} r_{jk}^2 = \frac{1}{2n^2}\sum_{i=1}^{n}\sum_{j=1}^{n} r_{ij}^2 \quad \text{or,}$$

$$\frac{1}{n^2}\sum_{1\le i< j\le n}\sum r_{ij}^2$$

which proves Lagrange's theorem.

In view of Lagrange's theorem, Eq. (9.90) informs us that, for scattering from isolated polymer chains and, in general, from isolated objects of any shape,

$$k\left\langle s^2\right\rangle^{1/2} << 1 \rightarrow P(k) = \frac{I(k)}{I(0)} = \frac{S(k)}{n} = 1 - \frac{k^2}{3}\left\langle s^2\right\rangle \quad \text{(Guinier Law)} \qquad (9.92)$$

The mean squared radius of gyration $\left\langle s^2\right\rangle$ of labelled macromolecules in a melt can thus be readily determined from the k-dependence of the scattered intensity of neutrons at very low k values. Eq. (9.92) also forms the basis for determining the mean squared radius of macromolecules in solution through light scattering experiments. Common ways of plotting experimental scattering data to determine $\left\langle s^2\right\rangle$ are shown in Fig. 9.20.

The SANS experiments on labelled chains in amorphous polymer melts and glasses were very important in the history of polymer science, in that they confirmed Flory's

1943 *random coil hypothesis* for chain conformations in the amorphous polymer bulk. Here we include a very brief note on the content of this hypothesis and on its consequences for overall dimensions of polymer chains.

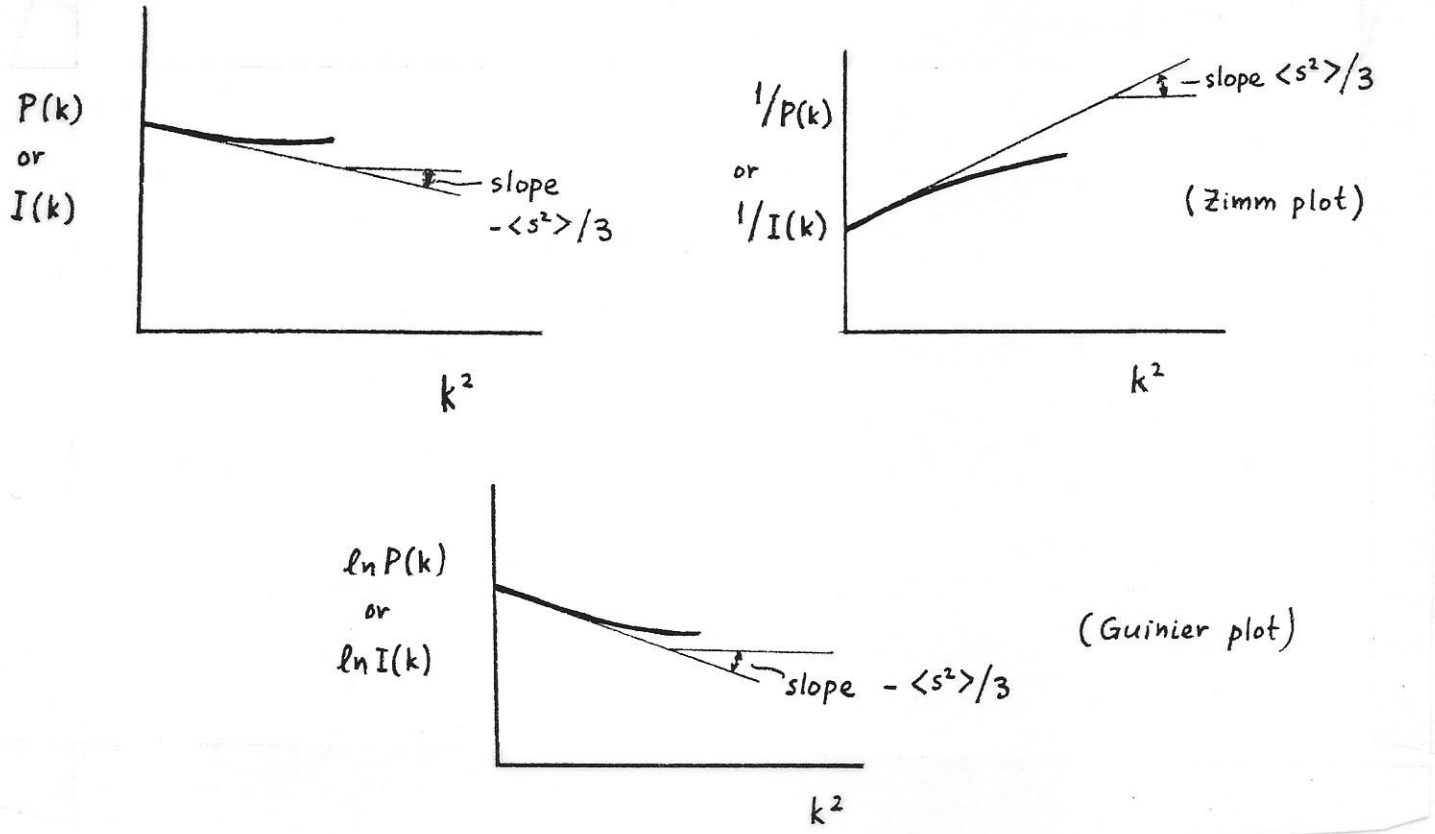

Figure 9.20 Common ways of plotting experimental scattering data from infinitely dilute systems of labelled polymer chains to extract the mean squared radius of gyration [compare Eq. (9.92)].

Interactions between mers of a polymer chain can be distinguished into two kinds: *local*, which involve mers that are only 3 or 4 bonds apart, and *nonlocal*, which occur between topologically distant mers as the chain curls back upon itself (see Fig. 9.21). Prominent in the nonlocal category are *excluded volume* interactions, arising from the

fact that no two segments can occupy the same position in space. Excuded volume interactions are responsible for the swelling of polymer coils in good solvents. According to the Flory random coil hypothesis [Flory (1953)], chain conformations in the amorphous bulk remain *unperturbed* by nonlocal interactions and are dictated only by local interactions along the backbone.

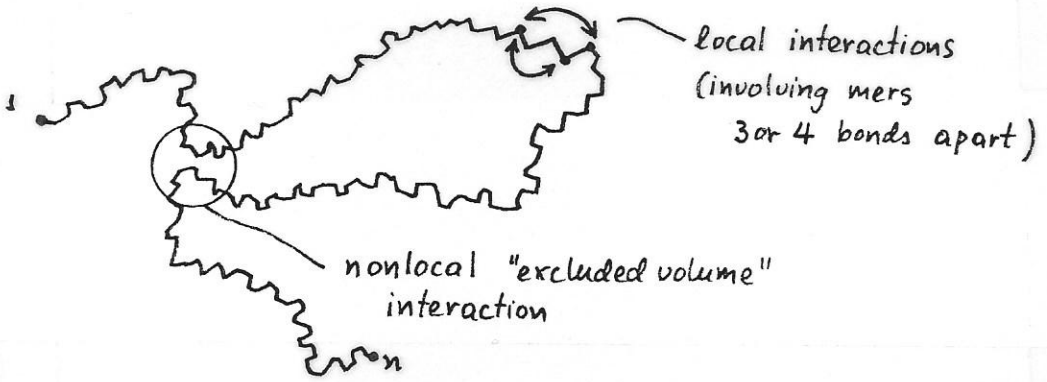

Figure 21 Schematic of a polymer chain, indicating local and nonlocal interactions

For an unperturbed chain of sufficient length $n >> 1$, the squared radius of gyration averaged over all conformations is proportional to the number of skeletal bonds. More specifically, the following relation holds between the mean squared end-to-end distance $\langle r_{1n}^2 \rangle$, the mean squared radius of gyration $\langle s^2 \rangle$, the number of bonds $(n-1)$, and the bond length ℓ:

$$\langle r_{1n}^2 \rangle = 6 \langle s^2 \rangle = C_\infty (n-1) \ell^2 \quad (n >> 1) \tag{9.93}$$

The constant C_∞ is called the *characteristic ratio* of the chain and depends on the chain chemical constitution and on temperature. C_∞ can be calculated from conformational

analysis of local interactions [Flory (1969)]; it constitutes a measure of the equilibrium conformational "stiffness" of the polymer coil.

The SANS experiments confirmed the relationship between mean squared radius of gyration and chain length predicted by Eq. (9.93), and thus validated Flory's random coil hypothesis experimentally. More recently, computer simulations of realistic models of short-chain polymer melts have shown that the random coil hypothesis provides an excellent approximation to intramolecular structure over all length scales.

The validity of Flory's random coil hypothesis greatly simplifies the calculation of the *intramolecular pair density function* $\omega(r)$, given the chemical constitution of a chain. Single unperturbed chains, subject only to local interactions, need be considered for this purpose. Accurate analytical treatments (*e.g.*, Rotational Isomeric State Model [Flory (1969)]) and Monte Carlo simulation techniques are available.

9.4.3 A note on Polymer RISM

The two previous sections addressed the question of intramolecular structure and chain conformation in melts. We now turn to the problem of calculating the *intermolecular pair distribution function* $g(r)$. As seen from Eq. (9.86), a knowledge of $g(r)$ is necessary for obtaining the total pair distribution function between mers, hence the thermodynamic properties of the melt.

The structure and thermodynamic properties of polymer melts can be predicted from the detailed geometry and energetics of chains using computer simulations, as we

shall see in Chapter 10. The application of traditional simulation techniques to polymer melts, however, is very compute-intensive, owing to the large length-scales and time-scales that characterize structure and motion in long-chain systems. Thus, there is much incentive for the development of analytical methods for calculating $g_{tot}(r)$ given the molecular geometry and interactions among mers. By Eq. (9.86), the calculation of g_{tot} calls for a knowledge of the intramolecular pair density function $\omega(r)$ and of the intermolecular pair distribution function $g(r)$. Of these, $\omega(r)$ can be obtained straightforwardly. As pointed out in section 9.4.2, Flory's random coil hypothesis reduces the problem of calculating $w(r)$ to one of accounting for all conformations of a single unperturbed chain; this is a manageable problem, even for very long chains, and theoretical and computational tools for dealing with it are in place. The problem of calculating $g(r)$ at given ρ and T once $\omega(r)$ is known is considerably more challenging. Here we will outline a promising integral equation theory approach for dealing with this problem.

In section 9.2 we discussed integral equation theories for obtaining $g(r)$ in simple fluids. These theories start with the Ornstein-Zernike equation (9.46), which they complement with a closure relation between $c(r)$ and $h(r)$. In Fourier - transformed space, the OZ equation for a simple fluid assumes the form

$$\hat{h}(k) = \hat{c}(k) + \rho\, \hat{c}(k)\, \hat{h}(k) \tag{9.47}$$

A simple graphical representation of the physical meaning of Eq. (9.47) is given in Fig. 9.22 (a): Molecules 1 and 2 are correlated because 1 and 2 are directly correlated, or because 1 is directly correlated to a third molecule 3, which is correlated with 2.

In a molecular fluid, molecules are represented as assemblages of atoms or *interaction sites.* An integral equation approach for molecular fluids known as the *Reference Interaction Site Model* (RISM) was developed by Chandler and Andersen [Chandler (1982)]. RISM starts from a set of Ornstein-Zernike - like equations relating the intermolecular pair correlation functions, the intramolecular pair density functions, and the direct intermolecular pair correlation functions for the different types of sites in the molecular system. Here we will not present the RISM formalism in its generality. We will only develop the RISM equations for the special case of a polyethylene melt consisting of one type of interaction sites (compare section 9.4.1).

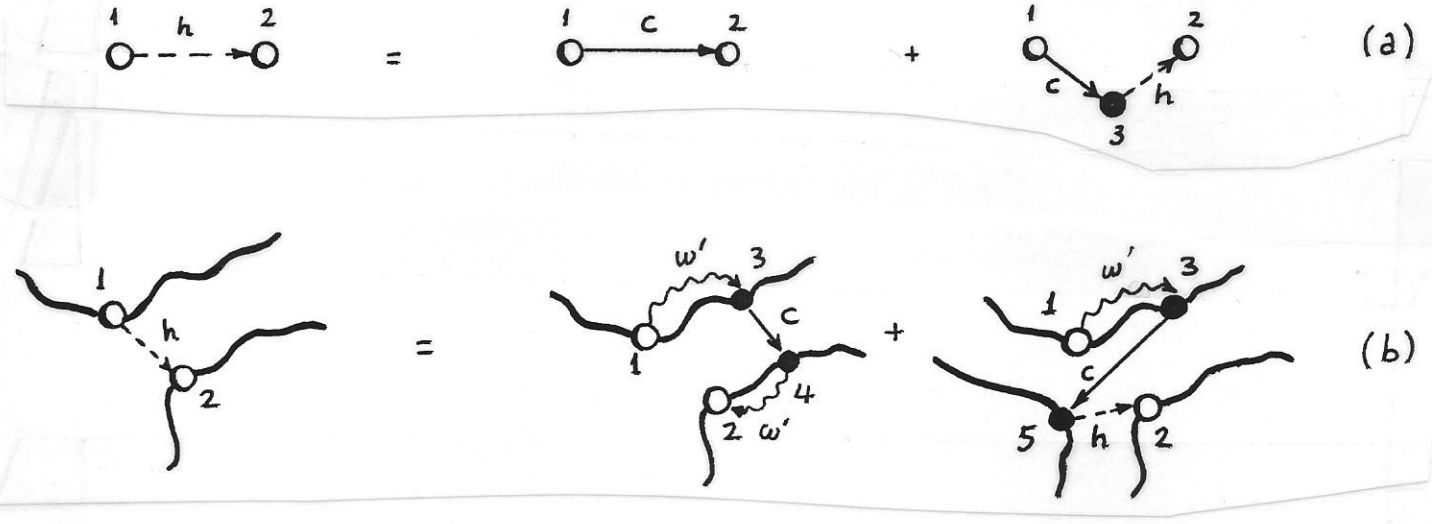

Figure 9.22 (*a*) Schematic interpretation of the OZ equation for a simple fluid. (*b*) Schematic interpretation of the RISM equation in a polymer melt.

Let $g(r)$ be the *intermolecular* mer - mer pair distribution function. The *intermolecular* pair correlation function $h(r)$ is defined, as usual, by $h(r) = g(r) - 1$. By our dis-

cussion in section 9.4.1, $h(r)$ will assume an asymptotic value of 0 at large distances. We introduce a direct *intermolecular* pair correlation function $c(r)$ between mers. Our objective is to write down an integral equation relating $h(r)$ to $c(r)$ and the intramolecular pair density function $\omega(r)$. This equation must express the total correlation between two segments 1 and 2 on two different chains. This correlation may be mediated by segments on the same chains as 1 and 2 [see segments 3 and 4 in Fig. 9.22 (b)], or on other chains [see segment 5 in fig. 9.22 (b)].

To express the RISM equation in a compact form, it is convenient to introduce the correlation function

$$\omega'(r) = \delta(\mathbf{r}) + \omega(r) \tag{9.94}$$

The intramolecular pair density function $\omega'(r)$ includes the effects of correlation of a reference mer *with itself*, as well as with other mers on its chain. The Fourier transform of $\omega'(r)$ is

$$\hat{\omega}'(k) = 1 + \hat{\omega}(k) \tag{9.95}$$

To develop the Polymer RISM equations, we think as follows [see Fig. 9.22 (b)]: Site 1 is correlated to site 2 because

(i) Site 1 is *intramolecularly* correlated to itself and other sites on its chain (3), which are *directly* correlated to sites (4) on the chain of 2, which are intramolecularly correlated to 2 or are the same as 2. This pathway of correlations contributes a term $\hat{\omega}'\,\hat{c}\,\hat{\omega}'$ to $\hat{h}(k)$.

(ii) Site 1 is *intramolecularly* correlated to itself and to other sites on its chain (3), which are *directly* correlated to sites (5) on *other chains* than the ones to which 1

or 2 belong. These other sites (5), in turn, are correlated to 2 through *total intermolecular correlations*. This pathway of correlations contributes a term $\rho\hat{\omega}'\,\hat{c}\,\hat{h}$ to $\hat{h}(k)$. Note that the mer density ρ comes into play here, as the probability of finding a segment 5 on a third chain to correlate through rises in proportion to the density.

The Polymer RISM equation in Fourier space is thus written

$$\hat{h}(k) = \hat{\omega}'(k)\,\hat{c}(k)\,\hat{\omega}'(k) + \rho\,\hat{\omega}'(k)\,\hat{c}(k)\,\hat{h}(k) \tag{9.96}$$

The real-space conterpart of Eq. (9.96) is

$$h(r_{12}) = \int \omega'(r_{13})\,c(r_{34})\,\omega'(r_{42})\,d^3r_3\,d^3r_4 + \rho \int \omega'(r_{13})\,c(r_{35})\,h(r_{52})\,d^3r_3\,d^3r_5 \tag{9.97}$$

The Polymer RISM equation can be supplemented with a closure relating h and c (*e.g.*, Percus-Yevick) to form an integral equation theory for the molecular system. Perturbation approaches analogous to the ones discussed in section 9.3 can be enlisted for dealing with the effects of mer-mer attractive interactions and for defining an equivalent hard-sphere diameter in lieu of the soft repulsive core of mers.

As an example of the Polymer RISM approach, we present some results for the structure of molten polyethylene obtained by Schweizer and Curro and their collaborators [Honnell *et al.* (1991)]. Their approach used a hard-sphere representation for mers, with an adjustable hard-sphere diameter d. The intramolecular pair density function $\omega(r)$ was estimated by invoking Flory's random coil hypothesis, based on the correct bonded geometry and local conformational energetics of chains (Rotational Isomeric State model enumeration with 500 cal/mol *trans* - *gauche* difference and 2000 cal/mol

pentane effect). The Percus-Yevick closure was employed in forming an integral equation theory out of the Polymer RISM equation. A monodisperse melt of chain length $n = 6,429$ was examined, and structural results were compared with X-ray diffraction measurements.

Figure 9.23 (a) shows the intermolecular pair distribution function $g(r)$ obtained by Polymer RISM for $d = 3.9$Å. The sharp cutoff at $r = d$ and the cusps observed around 5Å are a consequence of the hard-sphere representation of mers. In sharp contrast to the $g(r)$ functions we have discussed in conjunction with simple fluids, the intermolecular $g(r)$ in the polymer melt is lower than 1 throughout its domain, and approaches its asymptotic value of 1 only slowly. At small distances from the reference mer, one is likely to find mers belonging to the same chain as the reference mer. These same - chain mers exclude mers of other chains from coming close to the reference mer and lead to the depletion in intermolecular pairs observed in $g(r)$. This phenomenon is referred to as the "correlation hole" effect in the polymer literature. Clearly, the depression in $g(r)$ relative to 1 should be stronger the higher the molecular weight. The length scale of the "correlation hole" is commensurate with the mean squared radius of gyration of a chain. In this particular system, $\langle s^2 \rangle^{1/2} \simeq 130$Å.

Figure 9.23 (b) displays the Fourier transforms $\hat{\omega}(k)$ of the intramolecular pair density function and $\rho\,\hat{h}(k)$ of the intermolecular pair correlation function. Note that

$$\rho\,[g_{tot}(r) - 1] = \omega(r) + \rho\,h(r) \tag{9.98}$$

and therefore, by Eq. (9.29), the structure factor can be obtained as

$$S(k) - 1 = \hat{\omega}(k) + \rho\,\hat{h}(k) \quad \text{or}$$

$$S(k) = \hat{\omega}'(k) + \rho\,\hat{h}(k) \tag{9.99}$$

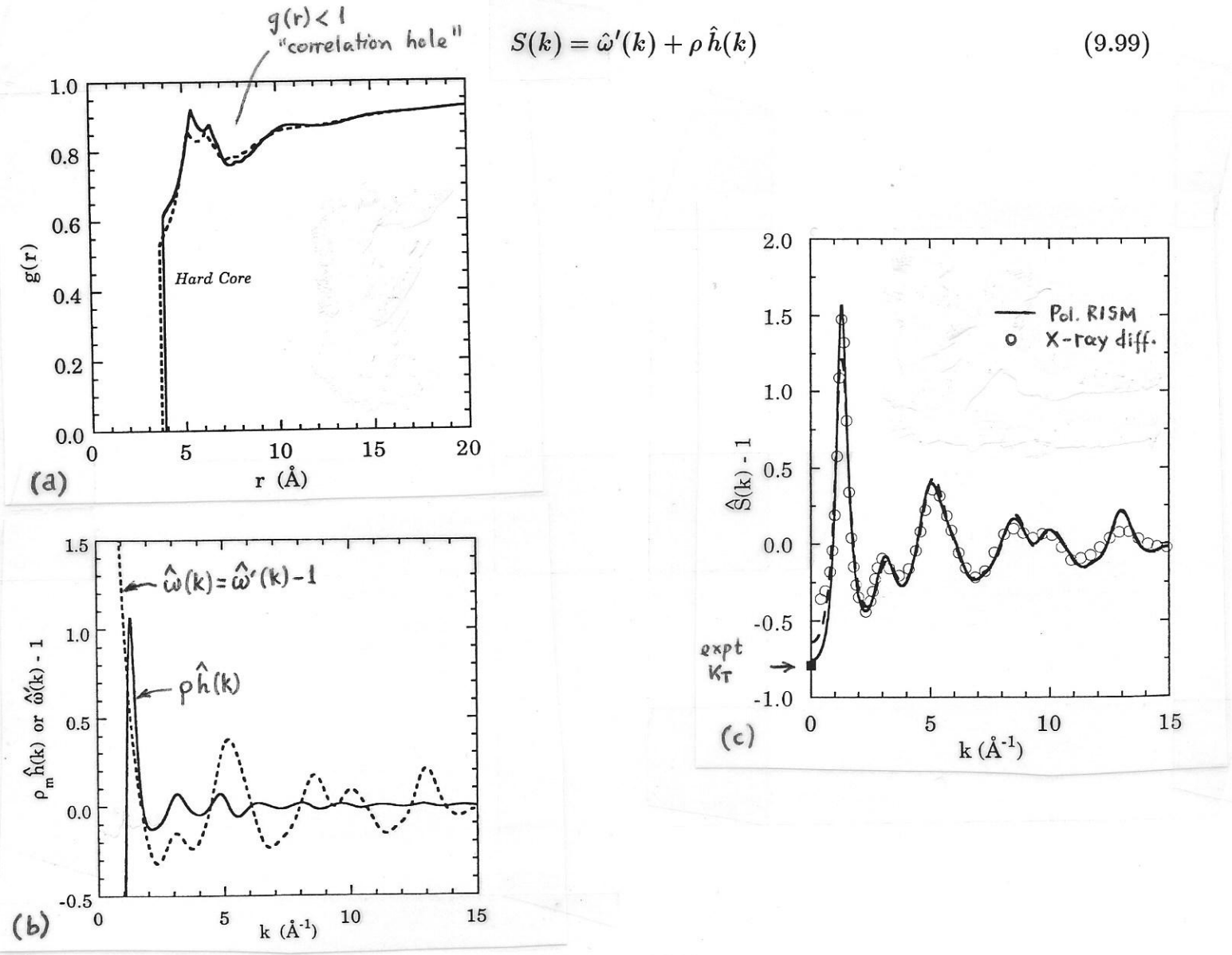

Figure 9.23 Results from application of the Polymer RISM formalism to a linear polyethylene melt [Honnell *et al.* (1991)]. (*a*) Intermolecular pair distribution function $g(r)$ for $\sigma = 3.9$Å (solid line). (*b*) Fourier transforms of intermolecular pair correlation function and intramolecular pair density function. (*c*) Structure factor, compared to experimental X-ray diffraction data.

The zero k limit of $\hat{\omega}'(k)$ is a direct consequence of the fact that $\int_0^\infty \omega(r) d^3r = n - 1$. Note also that, by Eq. (9.36),

$$S(0) = \hat{\omega}'(0) + \rho\,\hat{h}(0) = \rho k_B T \kappa_T \tag{9.100}$$

Thus, the small offset between the absolute values of $\hat{\omega}'(0)$ and $\rho\,\hat{h}(0)$ is a measure of the compressibility of the polymer melt. Intermolecular correlations contribute a strong peak (amorphous halo) around $k = 1.5$Å. This peak is directly related to the most probable distance between mers belonging to different chains in the bulk. Structural features at large k (small distances) are predominantly intramolecular, *i.e.*, due to the bonded geometry and conformational preferences of individual chains. The total structure factor is plotted in Figure 9.23 (c), along with experimental points from X-ray diffraction. The agreement between the $k = 0$ limit of the calculated $S(k)$ and the experimental isothermal conpressibility is partly fortuitous. In general, PVT predictions obtained with the RISM approach are not as successful as the structure calculations shown in Fig. 9.23.

References

Andersen, H.C., Weeks, J.D., Chandler, D. (1971). Relationship between the hard-sphere fluid and fluids with realistic repulsive forces. *Phys. Rev. A* **4**, 1597 - 1607.

Ballard, D.G., Schelten, J., Wignall, G.D. (1973). *Eur. Polym. J.* **9**, 965.

Carnahan, N.F. and Starling, K.E. (1969). Equation of state for nonattracting rigid spheres. *J. Chem. Phys.* **51**, 635-636.

Chandler, D. (1982). Equilibrium theory of polyatomic fluids. In Montroll, E.W., and Lebowitz, J.L. (Editors) *The liquid state of matter: fluids, simple and complex.* North Holland, Amsterdam.

Cotton, J.P., Decker, D., Bénoit, H., Farnoux, B., Higgins, J., Jannink, G., Ober, R., Picot, C., des Cloizeaux, J. (1974). Conformation of polymer chain in the bulk. *Macromolecules* **7**, 863 - 872.

Flory, P.J. (1953). *Principles of polymer chemistry.* Cornell University Press, Ithaca, N.Y.

Flory, P.J. (1969). *Statistical mechanics of chain molecules.* Wiley, NY.

Gillan, M.J. (1979) A new method of solving the liquid structure integral equations. *Molec. Phys.* **38** 1781-1794.

Hansen, J. P. and McDonald I. (1986). *Theory of simple liquids*, 2nd Ed. Academic Press, London.

Honnell, K.G., McCoy, J.D., Curro, J.G., Schweizer, K.S., Narten, A.H., Habenschuss, A. (1991). Local structure of polyethylene melts *J.Chem.Phys.* **94**, 4659-4662.

Hukins, D.W.L. (1981) *X-ray diffraction by disordered and ordered systems.* Pergamon Press, Oxford.

Kirste, R.G., Kruse, W.A., Schelten, J. (1973). Die Bestimmung des Trägerheitsradius von Polymethylmethakrylat im Glaszustand durch Neutronenbeugung. *Makromol. Chem.* **162**, 299 - 303.

McQuarrie, D. A (1976) *Statistical mechanics.* Harper and Row, New York.

Murrell, J.N., Boucher, E.A. (1982) *Properties of liquids and solutions.* Wiley, New York.

Page, D.I. (1973) The structure of liquids by neutron scattering. In Willis, B.T.M. (Editor) *Chemical applications of thermal neutron scattering.* Oxford University Press, Oxford, p 173-200.

Percus, J.K. and Yevick, J.G. (1958). Analysis of classical statistical mechanics by means of collective coordinates. *Phys. Rev.* **110**, 1 - 13.

Pings, C.J. (1970) Some current studies in liquid state physics. Part 1: Liquid state structure. *Chemical Engineering Education*, Winter 1970 issue, 18 - 23.

Press, W.H., Flannery, B.P., Teukolsky, S.A., Vetterling, W.T. (1986). *Numerical recipes.* Cambridge University Press, Cambridge.

Verlet, L. and Weis, J.-J. (1972). Equilibrium theory of simple liquids. *Phys. Rev. A* **5**, 939-952.

Weeks, J.D., Chandler, D., Andersen, H.C. (1971) Role of repulsive forces in determining the equilibrium structure of simple liquids. *J. Chem. Phys.* **54**, 5237 - 5247.